Copy
RM L58D16

NACA RM L58D16

NACA

RESEARCH MEMORANDUM

SOME FACTORS AFFECTING THE STABILITY AND PERFORMANCE CHARACTERISTICS OF CANARD AIRCRAFT CONFIGURATIONS

By M. Leroy Spearman and Cornelius Driver

Langley Aeronautical Laboratory
Langley Field, Va.

NATIONAL ADVISORY COMMITTEE
FOR AERONAUTICS

WASHINGTON

June 23, 1958

NATIONAL ADVISORY COMMITTEE FOR AERONAUTICS

RESEARCH MEMORANDUM

SOME FACTORS AFFECTING THE STABILITY AND PERFORMANCE CHARACTERISTICS OF CANARD AIRCRAFT CONFIGURATIONS

By M. Leroy Spearman and Cornelius Driver

SUMMARY

A survey has been made of some of the factors to be considered in the design of canard aircraft configurations. The factors include Mach number and angle-of-attack effects as well as the effects of various geometric changes. Among the geometric variables included are the effects of wing plan form, wing height, wing twist, canard plan form, canard area, canard moment arm, forebody length, afterbody length, forebody deflection, vertical-tail plan form, vertical-tail size, vertical-tail location, and various ventral-fin arrangements. The results indicate that generally acceptable longitudinal and directional stability characteristics can be obtained with canard configurations throughout a wide speed range from subsonic to supersonic speeds.

INTRODUCTION

Recent investigations have indicated that significant performance gains can be realized for airplanes at supersonic speeds by the use of canard controls rather than conventional tail-rearward controls. These gains include higher values of maximum lift-drag ratio and increased controllability. Because of these performance gains, an extensive research program was undertaken by the National Advisory Committee for Aeronautics for the purpose of determining the static stability and control characteristics of a number of canard airplane configurations. Various phases of the research program are reported in references 1 to 9, and some of the most recent canard airplane investigations are summarized herewith. The discussion is based primarily on results obtained in the Langley 4- by 4-foot supersonic pressure tunnel for Mach numbers of 1.41 and 2.01 although, for one configuration, some results are given for high subsonic speeds and for a supersonic Mach number range from 1.41 to 4.65.

SYMBOLS

The longitudinal stability characteristics are referred to the wind-axis system, whereas the lateral stability characteristics are referred to the body-axis system. The symbols are defined as follows:

C_L	lift coefficient, $\frac{\text{Lift}}{qS_w}$
C_D	drag coefficient, $\frac{\text{Drag}}{qS_w}$
C_m	pitching-moment coefficient, $\frac{\text{Pitching moment}}{qS_w\bar{c}_w}$
C_n	yawing-moment coefficient, $\frac{\text{Yawing moment}}{qS_wb}$
C_l	rolling-moment coefficient, $\frac{\text{Rolling moment}}{qS_wb}$
C_Y	side-force coefficient, $\frac{\text{Side force}}{qS_w}$
S_w	wing area including body intercept
S_c	canard-surface exposed area
b	wing span
c	local chord
t	thickness
$\bar{c}_w$	wing mean geometric chord
l_c	length between canard hinge line and center of gravity
q	free-stream dynamic pressure
M	Mach number

α	angle of attack, deg (positive, nose up)
β	angle of sideslip, deg (positive, nose left)
δ_c	canard deflection with respect to body center line, deg (positive, trailing edge down)
δ_f	trailing-edge flap deflection, deg (positive, trailing edge down)
δ_n	forebody deflection, deg (positive, nose up)
C_{n_β}	directional stability parameter, $\frac{\partial C_n}{\partial \beta}$ per deg
C_{l_β}	effective-dihedral parameter, $\frac{\partial C_l}{\partial \beta}$ per deg
C_{Y_β}	side-force parameter, $\frac{\partial C_Y}{\partial \beta}$ per deg
$\frac{\partial C_m}{\partial C_L}$	static longitudinal stability parameter
C_{m_δ}	canard pitching effectiveness, $\frac{\partial C_m}{\partial \delta_c}$ per deg
C_{L_δ}	canard trim-lift effectiveness, $\frac{\partial C_{L,trim}}{\partial \delta_c}$
L/D	lift-drag ratio
C_{L_α}	lift-curve slope, $\frac{\partial C_L}{\partial \alpha}$ per deg
$\frac{S_c l_c}{S_w \bar{c}_w}$	canard volume coefficient
A	aspect ratio
λ	taper ratio

Model Components and Subscripts:

B	fuselage (body)
W	wing
V	vertical tail
C	canard surface
U	ventral fin
max	maximum
min	minimum
o	conditions at zero lift

MODELS

Most of the results were obtained from tests of a variable-geometry general research model. Details of the various interchangeable components for the research model are shown in figures 1(a) to 1(d). The components, which included 5 bodies, 4 wings, 5 canard surfaces, 5 vertical tails, and 3 ventral fins are identified by a number subscript. Coordinates for the various body arrangements for the research model are presented in table I. Each wing (fig. 1(a)) was located with the trailing edge of the theoretical center-line wing root section coincident with the body base with the exceptions of W_3, which had its trailing edge located 1.3 inches forward of the base, and the configuration, with body B_2, for which a 5-inch body extension was added rearward of the wing—trailing-edge juncture. Each of the vertical tails (fig. 1(b)) and ventral fins (fig. 1(d)) were located so that the trailing edge of the exposed root sections were coincident with the body base (or the wing trailing edge in the case of wing-mounted surfaces) with the exception of the configuration with body B_2 for which a five-inch extension was added rearward of the tail and ventral trailing-edge juncture. Each of the canard surfaces (fig. 1(c)) were located with the hinge-line 9.125 inches rearward of the body nose. Spanwise locations for twin vertical-tail arrangements are noted in figure 1(a).

Some results were also obtained for a swept-wing model with various canard surfaces. Details of the swept-wing model are shown in figure 1(e), and coordinates for the body are presented in table II. A photograph of one of the research model configurations is shown in figure 1(f).

DISCUSSION

Longitudinal Stability and Trim Characteristics

Effects of Mach number.- The variations of some longitudinal aerodynamic parameters with Mach number for several canard airplane arrangements are shown in figure 2. These arrangements provide a limited comparison of wing plan-form effects and of afterbody effects. With the exception of some unpublished results for the extended afterbody at supersonic speeds, the results shown in figure 2 are contained in reference 1 for the supersonic range and in reference 2 for the subsonic range.

In comparison with the increase in longitudinal stability $\frac{-\partial C_m}{\partial C_L}$ usually experienced by conventional tail-rearward airplanes in passing through the transonic range, only a moderate increase in stability is indicated for the canard arrangements. This reduction in stability change through the transonic range is partially accomplished through the elimination of the afterbody and the conventional rearward horizontal tail so that the lift carry-over effects of the wing on the afterbody and the downwash changes at the tail are avoided. Thus the benefits of a relatively low stability level could be realized at supersonic speeds while still maintaining positive static stability at subsonic speeds. With the center of gravity at a constant body station, the stability level for the trapezoidal-wing configuration is higher than for the delta-wing configuration, primarily because the trapezoidal wing has the higher lift-curve slope. In addition, the increase in stability through the transonic range is somewhat greater (about -0.05) for the trapezoidal-wing configuration than for the delta-wing configuration.

While the addition of the extended afterbody had little effect on the subsonic stability level, its presence resulted in an additional increase in stability level at supersonic speeds because of the concentration of the wing-lift carry-over effects on the afterbody. The addition of the extended afterbody had no measurable effect on any of the other longitudinal aerodynamic parameters.

Although the two wings have the same area, the trapezoidal wing, by virtue of its higher aspect ratio, provides a higher lift-curve slope throughout the Mach number range, whereas the delta wing, by virtue of its higher leading-edge sweep and slightly lower thickness ratio, provides a lower drag rise and a lower minimum drag at supersonic speeds. As a result of the compensating effects of lift-curve slope and minimum drag, the two wing arrangements provide essentially the same maximum

untrimmed L/D at supersonic speeds. However, for a constant center-of-gravity position the trapezoidal-wing configuration has a higher static margin than the delta-wing configuration and would thus suffer larger losses in L/D because of trimming. For equal static margins, the trimmed L/D for the two configurations would be comparable; however, for equal static margins, the center-of-gravity position would be farther rearward for the trapezoidal-wing configuration than for the delta-wing configuration, and other factors such as the effect of center-of-gravity position on directional stability must be taken into consideration.

The longitudinal stability characteristics throughout a large Mach number range for the canard configuration with the trapezoidal wing and no afterbody are shown in figure 3. The results shown were extended to the higher supersonic Mach numbers from unpublished results of tests made in the Langley Unitary Plan wind tunnel. These results indicate a relatively constant value of untrimmed maximum L/D throughout the supersonic speed range. The static stability parameter $\partial C_m/\partial C_L$ indicates a progressive decrease in stability throughout the supersonic range, with the canard surface either on or off. As the stability decreases with increasing Mach number, the losses in maximum L/D caused by trimming also decrease. For the particular configuration illustrated (fig. 3), the stability level could be reduced to zero at the highest Mach number obtained ($M = 4.65$) and a static margin of about 8 percent mean aerodynamic chord at subsonic speeds could still be maintained.

Some remarks concerning the take-off and landing characteristics for the configuration shown in figure 3 might be of interest. Low-speed results (ref. 2) indicate that, for a static margin of about 8 percent $\bar{c}$, a trim lift coefficient of about 0.6 could be obtained at an angle of attack of about 10°. Other results presented in reference 2 indicate that the control effectiveness and maximum value of trimmed lift could be significantly increased by the addition of a conical-shaped body flap located slightly behind the canard on the bottom of the body.

Effects of canard surface size.- The effects of varying canard-surface size are of interest from a number of viewpoints. For a fixed center-of-gravity position, for example, the canard surface may be sized to provide a desired stability level. In addition, increases in canard size may be useful in providing higher lifts and higher maneuvering capability. On the other hand, the canard surface should not become so large that it precipitates a pitch-up condition, adversely affects inlet flow, or develops a wake of such intensity as to cause losses in total lift or in directional stability.

Some effects of canard-surface size on the longitudinal aerodynamic characteristics of a swept-wing configuration (fig. 1(e)) at $M = 1.41$

and of a delta-wing configuration at $M = 2.01$ are shown in figures 4 and 5, respectively. In general, the addition of the canard surface and the progressive increase in canard-surface area causes a progressive decrease in longitudinal stability but a decrease in maximum L/D is caused by the increase in minimum drag.

The effects of canard-surface size on the trimmed longitudinal characteristics of the delta-wing configuration at $M = 2.01$ are shown in figure 6 for a constant center-of-gravity position and in figure 7 for a constant static margin. For a constant center-of-gravity position the effect of increasing the canard-surface area is to cause a substantial increase in the variation of trim lift with control deflection $C_{L_{\delta,trim}}$ and a general increase in trimmed L/D. The increase in L/D is caused almost entirely by the reduction in stability that accompanies the increase in canard size. The increase in the variation of trim C_L with δ_c is caused by both the reduction in stability and the increase in control pitch effectiveness C_{m_δ} that accompanies the increase in canard size.

For a constant static margin (fig. 7), a comparison of the configurations with the smallest and the largest canard surfaces tested indicates only a slightly higher L/D for the large canard arrangement. Although there is considerably less difference in $C_{L_{\delta,trim}}$ between the two arrangements than there was for the case where the center of gravity was constant, the configuration with the larger canard surface still maintains a higher value of $C_{L_{\delta,trim}}$ because of its higher pitch effectiveness C_{m_δ}.

The variations of experimental and estimated values of C_{m_δ} and $\partial C_m/\partial C_L$ with canard-surface volume coefficient for the 60° delta-wing configuration at $M = 2.01$ are presented in figure 8. The estimated values do not include the effects of the canard-surface flow field on the wing. In general, the experimentally determined variations of C_{m_δ} and $\partial C_m/\partial C_L$ with canard-surface volume coefficient are in good agreement with the estimated variations.

As pointed out in reference 3, the longitudinal stability level may be more effectively changed by moving the center-of-gravity position than by varying the canard area. However, in order to provide a lower stability level for a given canard-surface size, it would be necessary to shift the center of gravity rearward, and the effect of such a shift on the directional stability may become a limiting factor.

Effect of wing twist.- The use of twist as a means of improving the drag due to lift of wings is well known. An additional feature of wing twist, of interest in the trimming problem, is the effect of twist on $C_{m,o}$. These effects are illustrated in figure 9 for a swept-wing configuration at $M = 1.41$ wherein the use of twist (4° linear washout from root to tip) produced a small reduction in drag due to lift, a small increase in maximum L/D, and a substantial positive increment in pitching moment throughout the lift range. It is this positive increment in pitching moment that is of primary interest for reducing trim L/D losses since a positive trim lift is obtained at zero control deflection, and the control deflections required for trimming at a given lift are thereby reduced.

These effects of wing twist on the control deflections required for trim and on the trim L/D are shown in figure 10. Because of the smaller control deflections required, the reductions in L/D caused by trimming are less and the maximum L/D is considerably higher with the twisted wing than with the plain wing.

Effect of forebody deflection.- The use of a cambered fuselage or a deflectable forebody offers another means of providing positive increments of pitching moments with little increase in drag and hence should be useful in reducing the pitch-control trimming requirements and the attendant losses in L/D due to trimming (see ref. 10).

Some effects of a deflected forebody on the trim longitudinal characteristics of a high-wing canard airplane arrangement at $M = 2.01$ are shown in figure 11. For this configuration, deflection of the forebody caused no change in static margin but did produce positive increments of pitching moment throughout the lift range. Therefore, deflection of the forebody resulted in substantial increases in trim lift for a given control deflection and increased the values of L/D at the higher lifts. In addition, a small increase in maximum L/D was indicated when the forebody was deflected.

Effects of wing height.- The effects of wing vertical location on the trim longitudinal characteristics of a trapezoidal-wing canard configuration at $M = 2.01$ (fig. 12) are quite small. The slightly higher values of L/D obtained with the low wing at high lifts is some indication of less influence of the canard-surface wake for the low wing than for the high wing. The results shown in figure 12 are for a configuration in which the wing is mounted on a cylindrical section of the fuselage. It is possible that the effects of wing height on the longitudinal stability characteristics may be more significant for configurations in which the fuselage is tapered in the vicinity of the wing.

Effects of body length.- The effects on trim longitudinal characteristics of varying the body length forward of the wing position are shown in figure 13 for a trapezoidal-midwing configuration at $M = 2.01$. The canard surface remained in the same position with respect to the nose and hence, with respect to the wing, moved forward as the body length increased. Varying the body length had little effect on L/D. The most significant effect of body length is apparent in the controllability wherein the variation of trim lift with control deflection increases as the body length increases. This effect, of course, is a result of the increased pitching effectiveness of the canard control that occurs as the canard-surface moment arm increases. Since the results are compared on the basis of equal stability levels for the three body lengths, it is required that the center-of-gravity position move forward, with respect to the wing, as the body length increases. However, the forward shift in center-of-gravity position is small when compared with the forward movement of the canard surface and an increase in canard moment arm occurs as the body length increases.

Effect of wing plan form.- Some effects of wing plan form on trim longitudinal characteristics at $M = 2.01$ are shown in figure 14 for high wing configurations having wings of equal area with either a trapezoidal or a 70° delta plan form. It is apparent that the 70° delta-wing configuration results in a lower trim C_{L_α} and $C_{L_{\delta_c}}$, a higher drag due to lift, and lower values of L/D through most of the lift range. The change in wing plan form affected the trim longitudinal characteristics for two primary reasons: (1) the differences in lift-curve slope and in induced drag resulting from the change in aspect ratio, and (2) the differences in canard-surface pitching effectiveness resulting from changes in interference effects from the wing. The effects of wing aspect ratio are obvious. The wing interference effects stem from a change in lift over the inboard portion of the wing that is caused by the flow field from the canard surface. Deflection of the canard surface for trimming (positive deflection or leading edge up) results in some loss in lift over the inboard portion of the wing. For the trapezoidal wing, this loss in lift occurs rearward of the center of gravity and results in a pitching-moment increment that is in the same direction as that produced by the canard surface. For the 70° delta wing, a considerable portion of the wing-root section is forward of the center of gravity, and the loss in lift induced by canard deflection results in a pitching-moment increment opposed to that caused by the canard. A similar effect is noted in reference 1. As a result of the wing interference effects, the pitching effectiveness for the delta-wing configuration is less than for the trapezoidal-wing configuration. In addition, for equal levels of static stability, the center of gravity is farther forward for the delta-wing configuration and this further reduces the canard-control pitch effectiveness. Therefore, a larger control deflection is required to trim at a given lift for the delta-wing configuration than for the

trapezoidal-wing configuration, and the result is an additional increase in trim drag.

For the same static margin the delta-wing configuration, in comparison with the trapezoidal-wing configuration, would permit greater center-of-gravity travel because of its greater $\bar{c}$. However, the general effects of wing plan form are essentially unchanged for the two configurations, even when compared at 0 static margin, since unpublished results indicate values of maximum L/D of 6.1 for the trapezoidal wing and 5.3 for the delta wing.

Effect of canard-surface plan form.- Some effects of canard-surface plan form on trim longitudinal characteristics at $M = 2.01$ are shown in figure 15 for 70° delta-midwing configurations having canard surfaces of equal exposed areas with either a trapezoidal or 70° delta plan form. The primary effect of canard-surface plan form is noticed in the controllability wherein the variation of $C_{L,trim}$ with δ_c is much less with the 70° delta canard surface than with the trapezoidal canard surface. This effect might be expected because of the lower aspect ratio and lift-curve slope for the 70° delta plan form.

Longitudinal Control

Comparison of canard control and trailing-edge flap control.- A comparison of the longitudinal trim characteristics of a 60° delta-wing configuration with canard controls and with wing trailing-edge flap controls is presented in figure 16 for a constant static margin of about 22 percent $\bar{c}$. These results indicate that the canard control, in comparison with the flap control, provides a higher trim lift-curve slope, a higher maximum trim lift, a lower drag due to lift, and a higher maximum L/D. The advantages of the canard control, when trimming is considered, stem not only from the longer moment arm but also from the fact that the canard control makes use of a positive lift increment for trimming. On the other hand, deflection of the trailing-edge flap for trimming produces a decrement in lift that must be made up through an increase in angle of attack, and thus the drag is increased and the L/D reduced.

Flap-control results are shown for the configuration with the canard surface off as well as with the canard surface installed at zero deflection (fig. 16). While the presence of the canard surface has only a small effect on the trim longitudinal characteristics, the use of the canard surface as a destabilizer permits a farther forward center-of-gravity position for a constant static margin and thus provides a longer moment arm not only to the pitch control but to the directional stability and control surfaces as well.

The configuration with the canard surface removed has a lower minimum drag that does result in slightly higher values of L/D at very low lifts and small flap deflections. This advantage, however, is quickly lost as the flap deflection increases.

The advantages of the canard control over the flap control in improving longitudinal trim characteristics would be less for lower stability levels. A comparison of the canard-control configuration with the flap-control tailless configuration (canard off) for a static margin of 10 percent $\bar{c}$ is shown in figure 17. The configuration with the canard control still provides a higher maximum lift and maximum L/D although the differences are less than those shown in figure 16 for a higher static margin.

Canard control and trailing-edge flap combination.- The use of plain trailing-edge flaps in conjunction with a canard control has been investigated for a 60° delta-wing configuration at M = 2.01 (figs. 18 and 19). For the trim longitudinal results shown in figure 18 the canard surface was considered as a trimmer fixed at various deflections while the flap was used as the pitch control. For the results shown in figure 19 the flap was considered as a trimmer and the canard surface was used as the pitch control. The primary benefit of the trailing-edge flaps, when deflected to provide trimming moments is to extend the trim lift range to higher values and thus provide a means for increasing the maneuverability. As previously pointed out, negative deflections of the flap cause a decrease in wing lift that must be made up through an increase in angle of attack, and thus the maximum value of L/D is reduced as the flap is deflected. While positive deflections of the flap would produce positive increments of lift and possibly increase the maximum L/D, the resulting increase in negative pitching moment that would have to be overcome with the canard control would place a restriction on the trim lift range and thus limit the maneuverability. The highest maximum trim value of L/D was obtained by use of the canard control alone when the trailing-edge flap deflection was zero. Only for a small lift range above the lift coefficient for maximum L/D did the use of the flap in conjunction with the canard control provide a higher L/D than that obtained with the canard control alone.

Comparison of canard control and deflected forebody control.- The control characteristics obtained with a deflected forebody are shown in figure 20 and those obtained with a deflected canard surface are shown in figure 21 for a configuration having a high-mounted trapezoidal wing at M = 2.01. The static margin near zero lift was about 11 percent $\bar{c}$ for each arrangement. The configuration with the deflected forebody control (fig. 20), because of its lower drag, provided a slightly higher value of maximum L/D than that obtained for the configuration with the canard control (fig. 21). In order to maintain equal static margins,

however, the center-of-gravity position for the deflected forebody configuration is located considerably farther rearward than that for the canard configuration. This far rearward center-of-gravity position not only contributes to the pitch-up indicated for the deflected forebody configuration but also places severe restrictions on the directional stability characteristics of the configuration.

Lateral and Directional Stability

Effect of vertical-tail size and location.- Some effects of vertical-tail size and location on the sideslip derivatives for a 60° delta-wing canard configuration at $M = 2.01$ are shown in figure 22. For the body-mounted tails (V_1 and V_2) there is a progressive decrease in $-C_{Y_\beta}$ and C_{n_β} with increasing angle of attack similar to that experienced by conventional airplane configurations (see ref. 10). These variations are probably caused by the effects of forebody, canard, and wing induced flow fields that produce sidewash changes as well as q changes at the tail. Increasing the size of the body-mounted tail (V_2 to V_1) only increases the magnitude of $-C_{Y_\beta}$ and C_{n_β} and does not alter the variations with angle of attack.

When the area of the large single tail (V_1) is replaced by a twin wing-mounted tail (V_3 or V_4) a considerable change occurs in the sideslip characteristics. Although the twin-tail arrangements V_3 and V_4 have the same tail volume as the single-tail arrangement V_1, there are substantial differences in the contributions of the tails to directional stability. The single body-mounted tail provides the largest contribution near $\alpha = 0°$ as a result, probably, of its height which places a large percentage of the tail area away from the disturbed flow fields of the body, wing, and canard surface. While both of the twin-tail arrangements provide less directional stability near $\alpha = 0°$ than the single tail of equivalent area, the effects of increasing angle of attack are much less severe for the twin tails than for the single tail. Of the two twin-tail arrangements, V_4 which is located at 50 percent of the wing semispan, provides higher values of C_{n_β} throughout the angle-of-attack range than V_3 which is located 25 percent of the wing semispan. The lower values of C_{n_β} for tail V_3 may result from the fact that this tail is located near the center of the wake from the canard surface, whereas tail V_4 is located outboard of the canard-surface wake and with increasing angle of attack probably benefits from a favorable sidewash.

Effect of canard surface.- The effects of the canard surface on the sideslip characteristics at $M = 2.01$ are presented in figure 23 for two of the configurations shown in figure 22. These configurations are with the small body-mounted tail V_2 and the outboard twin tails V_4. When the canard surface is added to the configuration having the single tail (fig. 23(a)), there is a general slight reduction in C_{n_β} with increasing angle of attack as an indication of the effects of the canard wake. However, when the canard surface is added to the configuration having the twin tails (fig. 23(b)), there is a general increase in C_{n_β} with increasing angle of attack as an indication of the favorable sidewash existing outboard of the canard wake.

The presence of the canard surface causes a general increase in the effective dihedral $\left(\text{more negative } C_{l_\beta}\right)$ for both tail arrangements. This is probably caused by a decrease in lift from the downwind wing panel resulting from the canard-surface wake.

As pointed out in reference 4, deflection of the canard control accentuates the wake effects from the canard surface in that C_{n_β} is generally further reduced for the single-tail arrangement and generally increased for the twin-tail arrangement. In addition, deflection of the canard control causes a further increase in $-C_{l_\beta}$ for both tail arrangements.

The effects of canard surfaces on sideslip derivatives cannot be completely generalized, however, and there is evidence that these effects vary considerably with Mach number and with various geometric variables such as wing plan form, wing position, body length, vertical-tail plan form, and so forth. Some effects of a canard surface on the sideslip derivatives at $M = 0.60$, 2.29, and 4.65 for a trapezoidal-wing configuration are shown in figure 24. Deflection of the canard for this configuration has a favorable effect on C_{n_β} at $M = 0.60$, particularly at higher angles of attack. The effect of the canard on C_{n_β} is less pronounced at $M = 2.29$ and varies from a slight favorable effect at low angles of attack to an adverse effect at high angles of attack. At $M = 4.65$ the effect of the canard on C_{n_β} is again favorable throughout most of the angle-of-attack range.

The effects of the canard surface on C_{l_β} for this configuration also show large variations with angle of attack and Mach number. These effects are primarily caused by an interference of the canard wake with

the wing and at $M = 4.65$, where the canard wake is confined by the Mach lines to a small cone, the effects on the wing are small.

The effects of canard-surface size ($\delta_c = 0^\circ$) on the sideslip characteristics at $M = 2.01$ are presented in figure 25 for the configurations shown in figure 8. For the configurations investigated, the effects of canard size on the sideslip characteristics were relatively small.

Effect of ventral fins.- The use of ventral fins on canard configurations might be expected to improve the directional stability in much the same manner as on conventional configurations. In addition, the arrangement of canard configurations is such that auxiliary fins mounted on the wing might also be incorporated as directional stabilizing devices. Such an arrangement employing either a lower-surface or an upper-surface wing-mounted fin is shown in figure 26 for a delta-wing configuration at $M = 2.01$. Both arrangments are effective in increasing C_{n_β}, but the lower-surface installation provides larger increases than the upper-surface installation at higher angles of attack. Neither arrangement causes any significant change in C_{l_β}.

An arrangement utilizing twin body-mounted ventral fins is shown in figure 27. The addition of these fins provides a substantial increment in C_{n_β} that increases slightly with increasing angle of attack. The addition of these fins also causes an increase in $-C_{l_\beta}$, regardless of the increased lateral area below the center of gravity. This effect is probably a result of an interference between the ventral fins and the wing panels.

Effect of forebody deflection.- Although the use of a deflected forebody offers some advantages in longitudinal control the effects of forebody deflection on the sideslip derivatives should also be considered. These effects are illustrated in figure 28 for the same configuration shown in figure 11. The most significant effect of forebody deflection is a more rapid deterioration of C_{n_β} with increasing angle of attack as the forebody is deflected upward. Similar effects were also found to occur for a low-wing configuration. Additional tests made with the vertical tail removed indicated that this effect was a result of a decrease in the tail contribution to C_{n_β} and, therefore, may not exist for a twin-tail arrangement and may, in fact, increase the effectiveness of twin tails.

Effect of strakes.- The use of forebody strakes has been shown to be an effective means of increasing the level of directional stability

at high angles of attack for a Mach number of 2.01 (see ref. 10). The use of a strake in conjunction with a canard surface has been investigated for a 60° delta-wing configuration at $M = 2.01$, and the effects on the sideslip derivatives are shown in figure 29. Although the addition of the strake provides some increase in C_{n_β} with increasing angle of attack, the effect is not so striking as that obtained with a strake on plain nose configurations. (See ref. 10, for example.) Apparently the interruption of the strake caused by the canard surface disrupts the effectiveness of the strake. This result suggests that a continuous strake along the forebody with the canard surface located outboard of the strake may be a more effective arrangement.

Effect of wing plan form.- The sideslip derivatives at $M = 2.01$ for two high-wing single-tail configurations with either a trapezoidal wing or a 70° delta wing are compared in figure 30. This comparison indicates a generally higher level of C_{n_β} for the 70° delta-wing configuration with the tail on regardless of an accompanying increase in the level of instability with the tail off. This effect, of course, indicates a considerable increase in the tail contribution for the delta-wing configuration that apparently results from a shielding of the vertical tail from the forebody vorticity. This effect is also apparent in the increased tail contribution to C_{l_β} and C_{Y_β} for the delta-wing configuration when compared with the trapezoidal-wing configuration.

Effect of wing height.- Some effects of wing height on the sideslip derivatives for a trapezoidal-wing configuration with and without a single tail at $M = 2.01$ are shown in figure 31. These results indicate a higher level of C_{n_β} at low angles of attack for the tail-on configuration with the low wing than with the high wing because of a substantially higher contribution from the vertical tail. With increasing angle of attack, the tail contribution to C_{n_β} decreases for both wing heights. However, because of a decrease in the tail-off instability with increasing α with the high wing, the variation in C_{n_β} with α with the tail on is less for the high wing than for the low wing. As a result, the value of C_{n_β} becomes zero at approximately the same angle of attack for both wings, and at higher angles of attack the high-wing configuration indicates a higher degree of stability than does the low-wing configuration.

These effects of wing height on C_{n_β} are similar to those observed for conventional airplane configurations for Mach numbers up to about 2 (refs. 10 to 12). As pointed out in these references, these effects

result from the induced sidewash from the wing-body juncture that provides a destabilizing flow above the high wing and a stabilizing flow below the high wing. An opposite effect occurs for the low-wing case. The effects of wing height on C_{n_β} appear to be more pronounced for the canard configuration (fig. 31) than the effects shown for the same wings at the same Mach number for a conventional tail-rearward airplane (ref. 12). This result might be expected since, for the canard configuration, the vertical tail is closer to the origin of the induced sidewash of the wing-body juncture.

The effects of wing height on the effective dihedral C_{l_β} for the canard configuration (fig. 31) are also similar to the effects observed for conventional configurations (ref. 12, for example) wherein the high-wing arrangement provides the greater dihedral effect (more negative C_{l_β}).

The effect of wing height on the sideslip derivatives at $M = 2.01$ for a 70° delta-wing configuration with either a single vertical tail or twin vertical tails is shown in figure 32. For the single-tail arrangement, the effects of wing height are, in general, similar to those observed for the trapezoidal-wing configuration (fig. 31). However, for the twin-tail arrangement, the effects of wing height on C_{n_β} are essentially opposite to those for the single tail inasmuch as the high-wing configuration provides a higher level of C_{n_β} throughout the angle-of-attack range than does the low-wing configuration. For the high-wing configuration, the twin-tail arrangement provides about four times as much directional stability as does the single-tail arrangement at $\alpha = 0^\circ$. This result suggests that there is a favorable interference effect on the tail contribution. For the low-wing configuration, however, the twin-tail arrangement provides about the same directional stability as the single-tail arrangement at $\alpha = 0^\circ$. This result suggests that there is an adverse interference effect on the contribution of the twin tail. This reversal in the effects of wing height on the tail contributions may result from the fact that the twin tails are located outboard of the region of the induced sidewash of the wing-body juncture; therefore, in the case of the low wing, for example, the twin tails may be in an adverse sidewash, whereas a single tail may be in a favorable sidewash. The opposite effect, of course, would exist for the high-wing case.

With increasing angle of attack, the flow interference from the low wing for the twin-tail arrangement apparently moves off the tails, and above $\alpha \approx 10^\circ$ the tail contributions to C_{n_β} are about the same for both wing positions. The level of C_{n_β} remains somewhat higher

for the high-wing arrangement, however, as a result of its tail-off characteristics.

The effects of wing height on the effective dihedral are essentially the same for the twin-tail arrangement as for the single-tail arrangements. The effect of the wing-body induced sidewash is apparent, however, inasmuch as the vertical-tail contributions to C_{l_β} for the twin-tail arrangement are less for the low wing than for the high wing, whereas the reverse is true for the single-tail arrangement.

Effects of body length.- Some effects of body length on the sideslip derivatives at $M = 2.01$ for a trapezoidal-midwing configuration with and without a single vertical tail are shown in figure 33. For these results, the center-of-gravity position was located in a fixed position with respect to the body base, and thus the percentage of body length forward of the center of gravity is increased as the body length increases. A direct effect of the increase in forebody length is apparent in the increase in directional instability with the tail off throughout the angle-of-attack range. This effect is also reflected in the directional stability levels with the tail on. In addition, as the forebody length is increased, the loss in tail contribution with increasing angle of attack becomes greater. This effect is associated with an upward displacement of the forebody-induced vorticity as the forebody length is increased.

It should be remembered that the longitudinal stability decreases as the forebody length is increased; therefore, for a constant static margin, the center-of-gravity location would move forward as the forebody length increases. This fact would result in an increase in the level of directional stability for the longer body configurations.

Effect of canard-surface plan form.- The effects of canard-surface plan form on sideslip derivatives at $M = 2.01$ are shown in figure 34 for 70° delta-midwing configurations having canard surfaces of either a trapezoidal or a delta plan form. The change in canard plan form had a relatively small effect on the sideslip derivatives, with the most noticeable difference being higher values of C_{n_β} at high angles of attack for the configuration with the 70° delta canard surface. This difference may be partly caused by a "strake" effect resulting from the long root chord of the delta canard and partly caused by a decrease in canard wake effects resulting from the lower lift-curve slope for the delta canard surface.

Mach number effects.- The variation of sideslip derivatives through a large Mach number range are presented in figure 35 for a trapezoidal-midwing configuration. This is the same configuration for which the

longitudinal characteristics are presented in figure 3. The results presented in figure 35 for $\alpha = 0^\circ$ and $\alpha = 6^\circ$ indicate positive directional stability and positive effective dihedral throughout the Mach number range investigated.

CONCLUDING REMARKS

A survey was made of some of the factors to be considered in the design of canard aircraft configurations. These factors include Mach number and angle-of-attack effects as well as the effects of various geometric changes. The results indicate that generally acceptable longitudinal and directional stability characteristics can be obtained with canard configurations throughout a wide speed range from subsonic to supersonic speeds.

The maximum values of trimmed lift-drag ratio L/D were increased through the use of such design features as wing twist and nose-up forebody deflection that provided positive increments of pitching moment with little change in drag. In addition, the values of maximum L/D were increased through the use of wings having high aspect ratios.

The control effectiveness was increased as the canard volume was increased either by an increase in canard area or forebody length, and through the use of canard surfaces having high aspect ratios.

The longitudinal-control characteristics indicated that higher trimmed values of lift-drag ratio were obtained with a canard control alone than with trailing-edge flap controls either alone or used in conjunction with the canard control.

The lateral and directional stability results indicated a wide variation in the effects of Mach number, angle of attack, and geometric design. For the most part the lateral and directional characteristics were similar to those for conventional aircraft and indicated that increased directional stability could be obtained through the use of such design features as ventral fins, short forebodies, and long wing-root chords. In addition, canard configurations are readily adaptable to twin vertical-tail arrangements, and results indicate that twin tails can be located to take advantage of favorable interference flow fields.

Langley Aeronautical Laboratory,
National Advisory Committee for Aeronautics,
Langley Field, Va., March 31, 1958.

REFERENCES

1. Driver, Cornelius: Longitudinal and Lateral Stability and Control Characteristics of Two Canard Airplane Configurations at Mach Numbers of 1.41 and 2.01. NACA RM L56L19, 1957.

2. Sleeman, William C., Jr.: Investigation at High Subsonic Speeds of the Static Longitudinal and Lateral Stability Characteristics of Two Canard Airplane Configurations. NACA RM L57J08, 1957.

3. Spearman, M. Leroy, and Driver, Cornelius: Effects of Canard Surface Size on Stability and Control Characteristics of Two Canard Airplane Configurations at Mach Numbers of 1.41 and 2.01. NACA RM L57L17a, 1958.

4. Spearman, M. Leroy, and Driver, Cornelius: Longitudinal and Lateral Stability and Control Characteristics at Mach Number 2.01 and a 60° Delta-Wing Airplane Configuration Equipped With a Canard Control and With Wing Trailing-Edge Flap Controls. NACA RM L58A20, 1958.

5. Boyd, John W., and Peterson, Victor L.: Static Stability and Control of Canard Configurations at Mach Numbers From 0.70 to 2.22 - Longitudinal Characteristics of a Triangular Wing and Canard. NACA RM A57J15, 1958.

6. Boyd, John W., and Peterson, Victor L.: Static Stability and Control of Canard Configurations at Mach Numbers From 0.70 to 2.22 - Triangular Wing and Canard on an Extended Body. NACA RM A57K14, 1958.

7. Peterson, Victor L., and Menees, Gene P.: Static Stability and Control of Canard Configurations at Mach Numbers From 0.70 to 2.22 - Longitudinal Characteristics of a Triangular Wing and Unswept Canard. NACA RM A57K26, 1958.

8. Peterson, Victor L., and Boyd, John W.: Static Stability and Control of Canard Configurations at Mach Numbers From 0.70 to 2.22 - Longitudinal Characteristics of an Unswept Wing and Canard. NACA RM A57K27, 1958.

9. Peterson, Victor L., and Menees, Gene P.: Static Stability and Control of Canard Configurations at Mach Numbers From 0.70 to 2.22 - Lateral Directional Characteristics of a Triangular Wing and Canard. NACA RM A57L18, 1958.

10. Spearman, M. Leroy: Some Factors Affecting the Static Longitudinal and Directional Stability Characteristics of Supersonic Aircraft Configurations. NACA RM L57E24a, 1957.

11. Spearman, M. Leroy, and Robinson, Ross B.: Investigation of the Aerodynamic Characteristics in Pitch and Sideslip of a 45° Swept-Wing Airplane Configuration With Various Vertical Locations of the Wing and Horizontal Tail - Static Lateral and Directional Stability; Mach Numbers of 1.41 and 2.01. NACA RM L57J25a, 1957.

12. Robinson, Ross B.: Effects of Vertical Location of the Wing and Horizontal Tail on the Static Lateral and Directional Stability of a Trapezoidal-Wing Airplane Model at Mach Numbers of 1.41 and 2.01. NACA RM L58C18, 1958.

TABLE I.- BODY COORDINATES FOR BODIES B_1, B_2, B_3, B_4, AND B_5

Body station	Radius
Forebody (all bodies)	
0	0
.297	.076
.627	.156
.956	.233
1.285	.307
1.615	.378
1.945	.445
2.275	.509
2.605	.573
2.936	.627
3.267	.682
3.598	.732
3.929	.780
4.260	.824
4.592	.865
4.923	.903
5.255	.940
5.587	.968
5.920	.996
6.252	1.020
6.583	1.042
Body, B_1	
18.648	1.75
37.000	1.75
Body, B_2	
18.648	1.75
42.000	1.75
Body, B_3	
17.75	1.667
31.50	1.667
Body, B_4	
17.75	1.667
37.00	1.667
Body, B_5	
17.75	1.667
41.50	1.667

TABLE II.- BODY COORDINATES FOR SWEPT-WING MODEL

Body station, in.	Radius, in.	
	Major axis	Minor axis
0	0	0
1	.297	.198
2	.492	.328
3	.655	.437
4	.799	.533
5	.928	.619
6	1.045	.696
7	1.151	.767
8	1.248	.832
9	1.337	.891
10	1.418	.945
11	1.492	.995
12	1.559	1.040
13	1.620	1.080
14	1.666	1.116
15	1.666	1.149
16	1.645	1.175
17	1.609	1.190
18	1.551	1.195
19	1.482	1.195
20	1.399	1.195
21	1.325	1.195
22	1.257	1.195
23	1.198	1.195
24	1.211	1.195
25	1.260	1.195
26	1.332	1.195
27	1.446	1.195
28	1.514	1.195
29	1.542	1.195
30	1.554	1.195
31	1.534	1.195
32	1.489	1.195
33	1.433	1.195
34	1.369	1.182
35	1.303	1.155
36	1.231	1.117
37	1.155	1.072
38	1.067	1.025
39	.975	.975

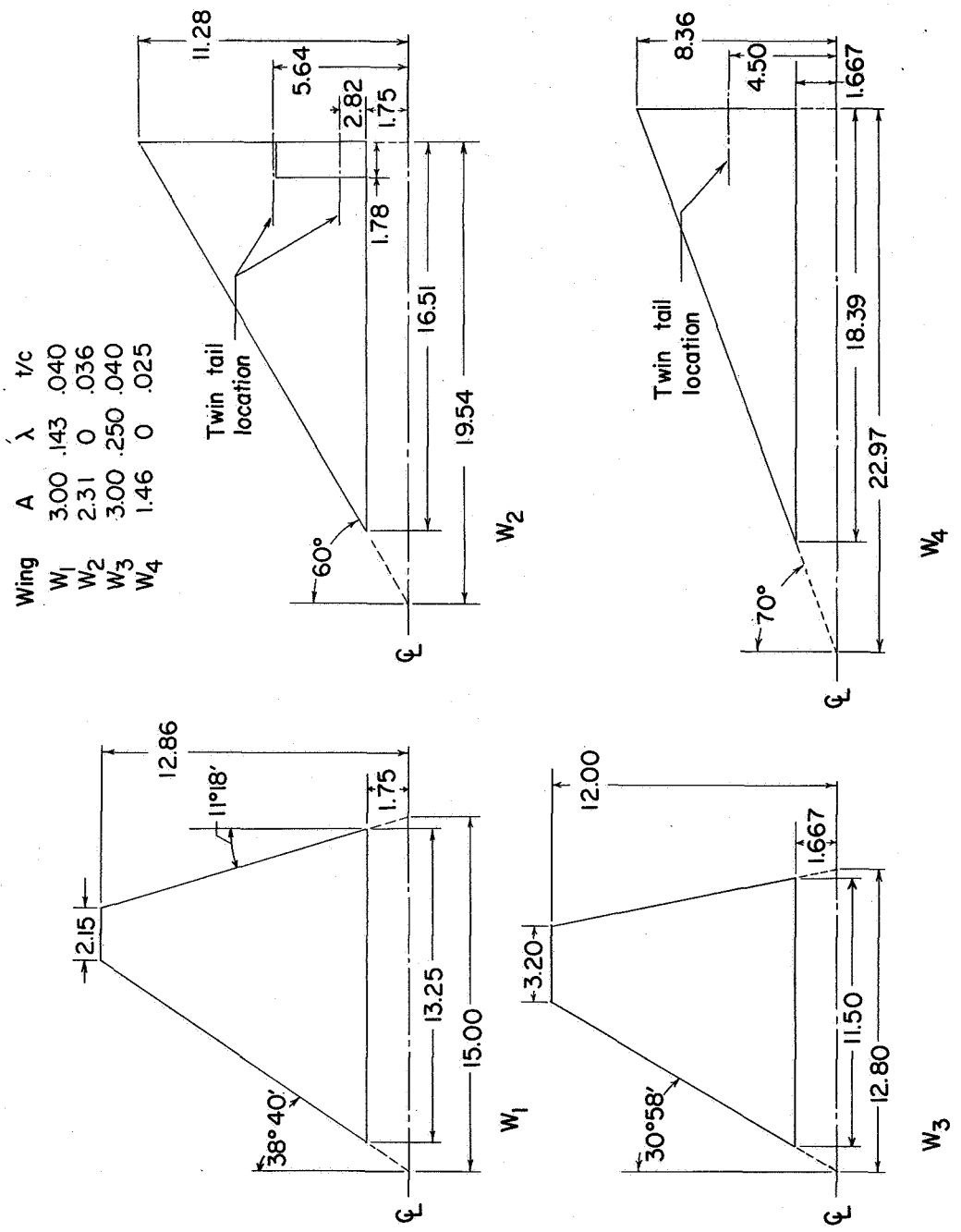

(a) Wings W_1, W_2, W_3, and W_4.

Figure 1.- Details of models. All dimensions in inches unless otherwise noted.

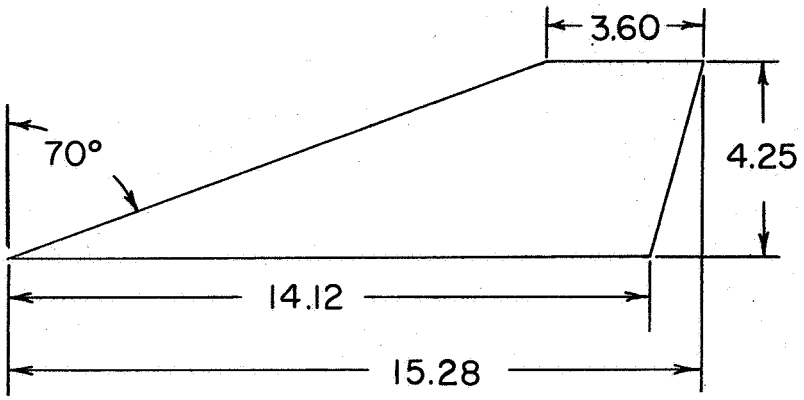

V_5

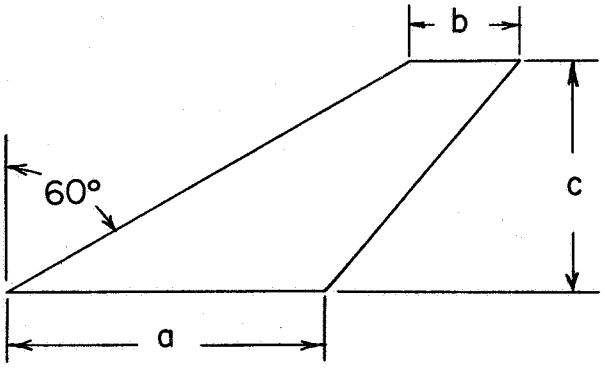

	V_2, V_3, V_4	V_1
a	7.00	10.05
b	2.20	3.16
c	5.10	7.20

(b) Vertical tails V_1, V_2, V_3, V_4, and V_5.

Figure 1.- Continued.

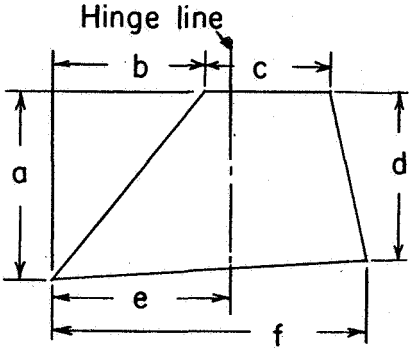

	C_1	C_2	C_3	C_4
a	2.25	2.25	2.64	2.90
b	1.80	1.80	2.11	2.32
c	1.50	2.15	2.38	2.54
d	2.03	2.00	2.35	2.59
e	2.13	2.34	2.88	3.13
f	3.73	4.34	4.95	5.38

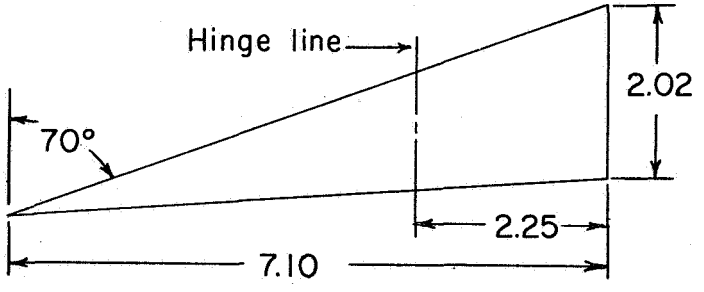

C_5

(c) Canard surfaces C_1, C_2, C_3, C_4, and C_5.

Figure 1.- Continued.

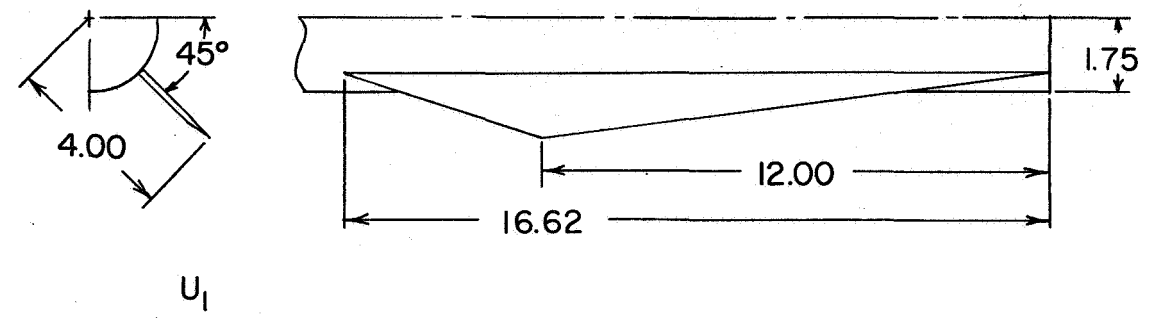

U_1

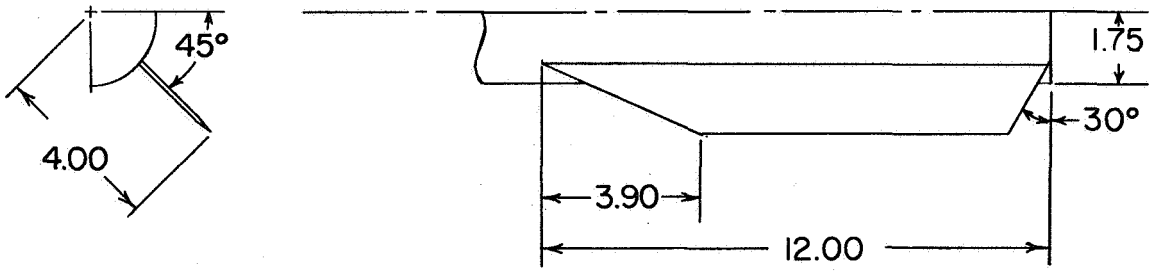

U_2

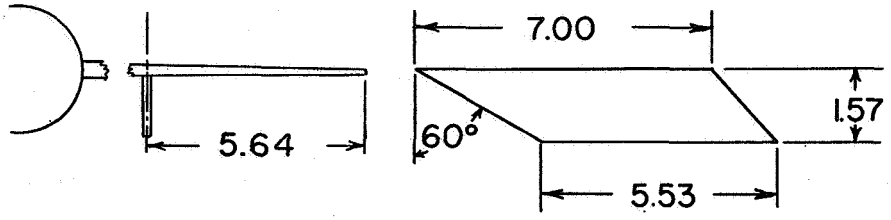

U_3

(d) Ventral fins U_1, U_2, and U_3.

Figure 1.- Continued.

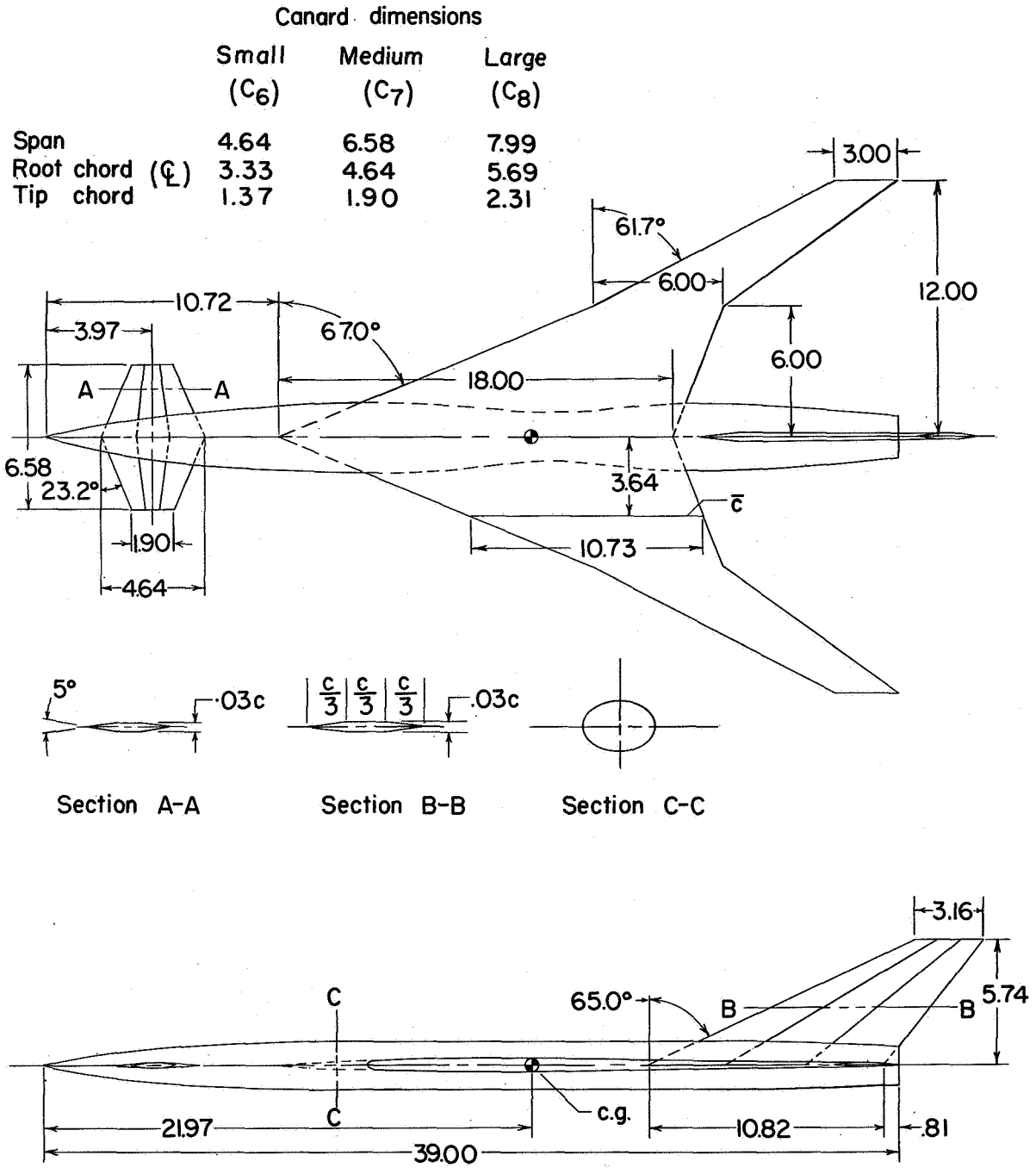

(e) Details of swept-wing model.

Figure 1.- Continued.

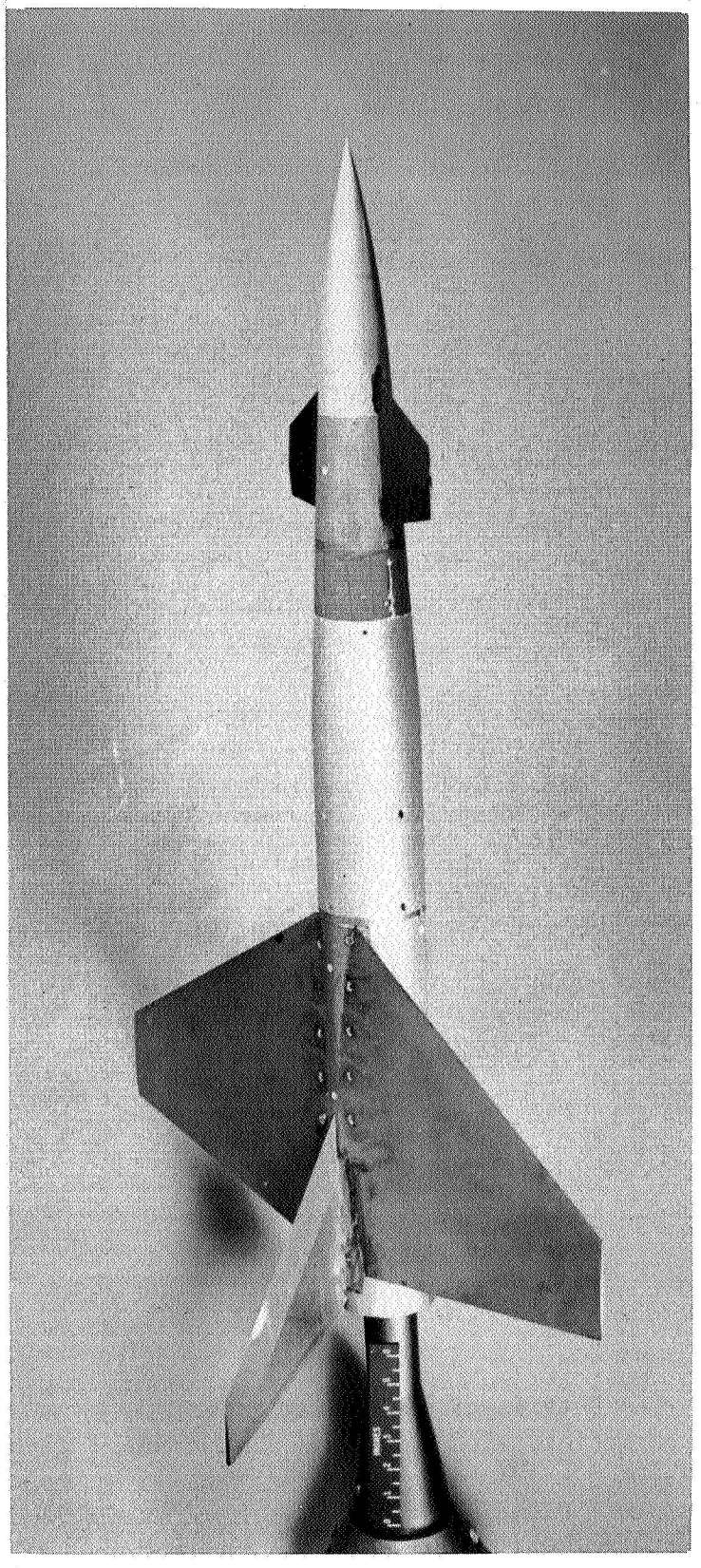

(f) Photograph of $B_4W_3V_2C_2$ model with high wing. L-57-2681

Figure 1.- Concluded.

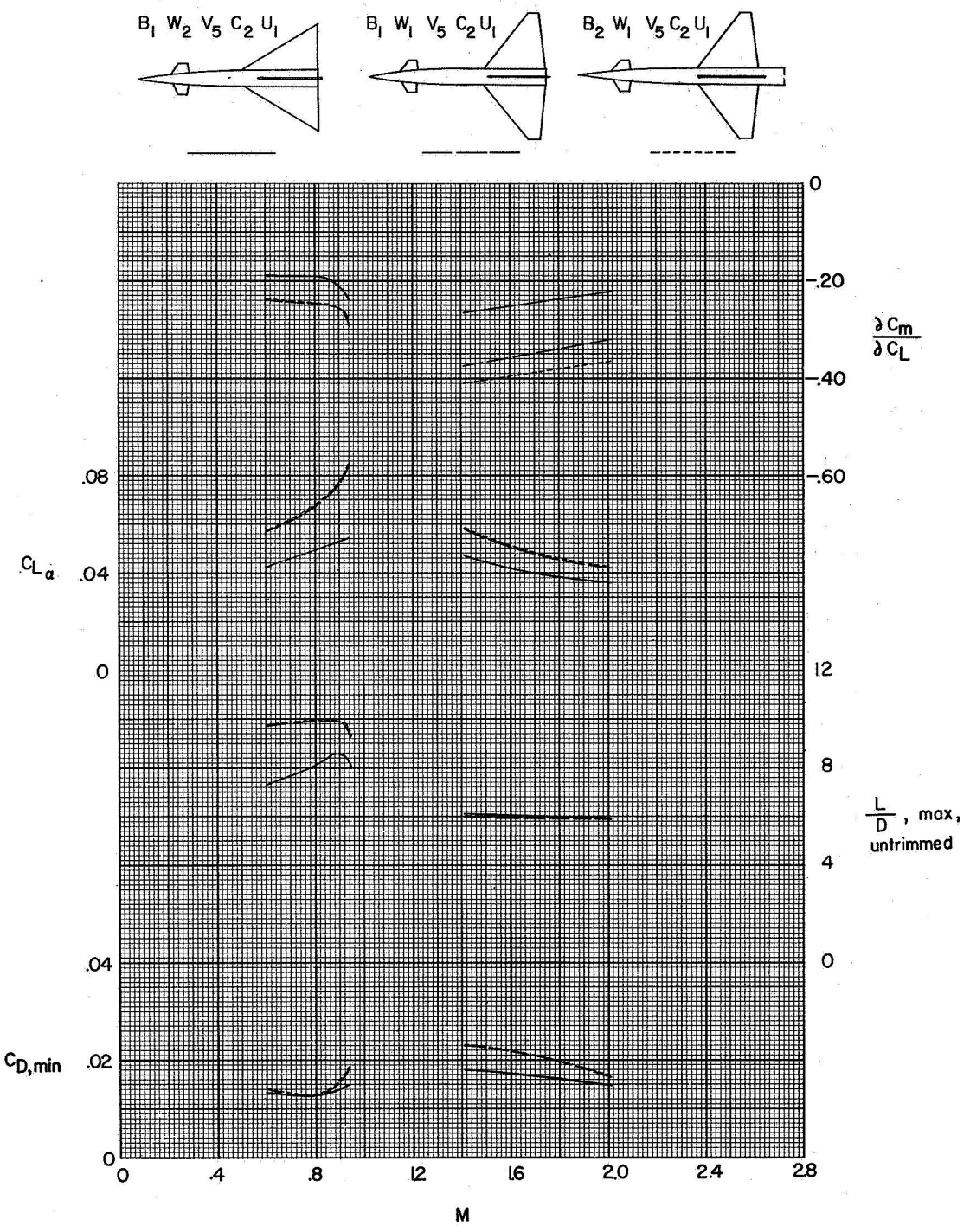

Figure 2.- Effect of wing plan form and fuselage afterbody on variation of longitudinal parameter, with Mach number. Center-of-gravity position of body station 25.

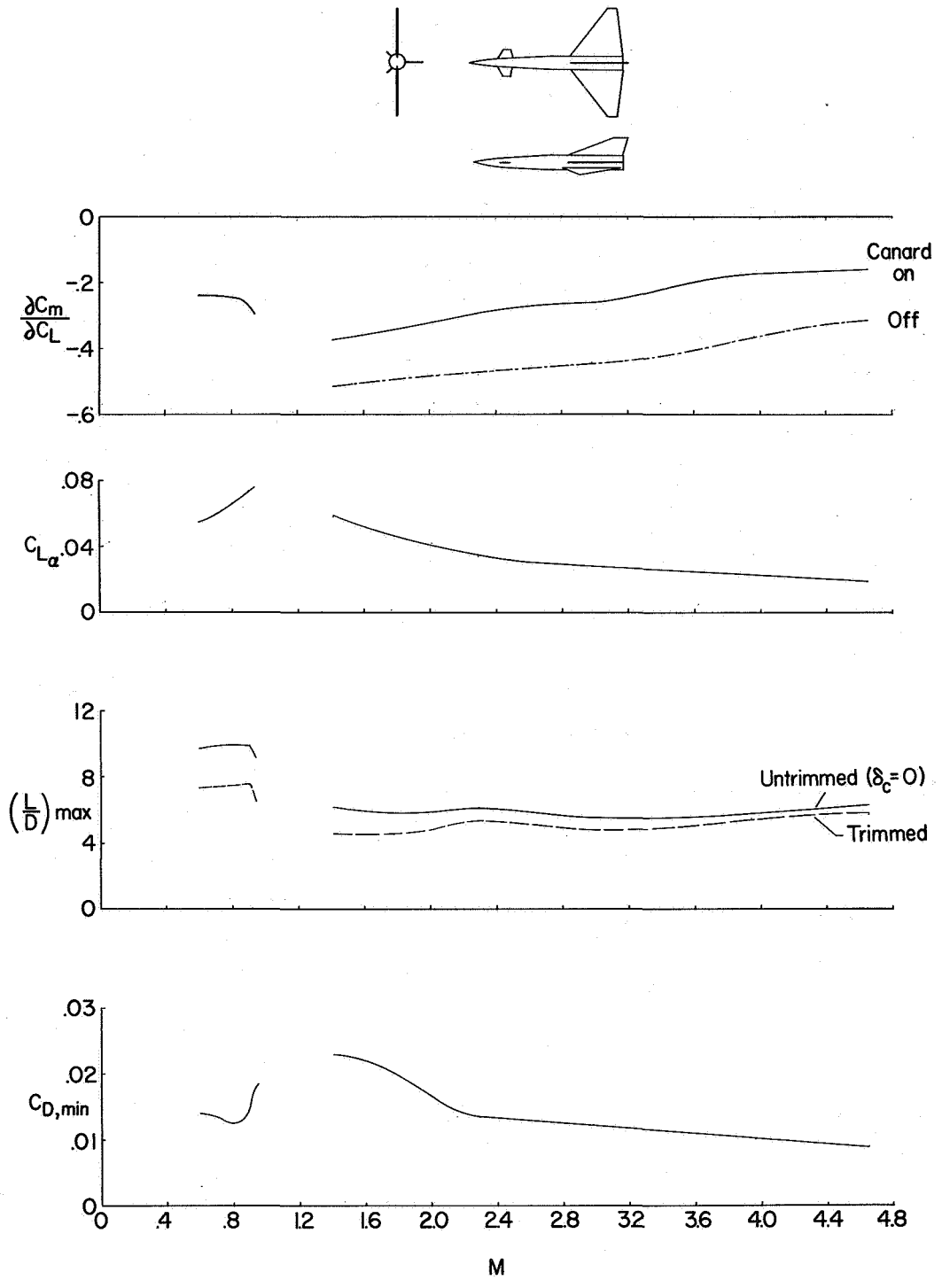

Figure 3.- Variation of longitudinal characteristics with Mach number for trapezoid-midwing configuration. $B_1W_1V_5C_2U_1$. Center-of-gravity position at body station 25.

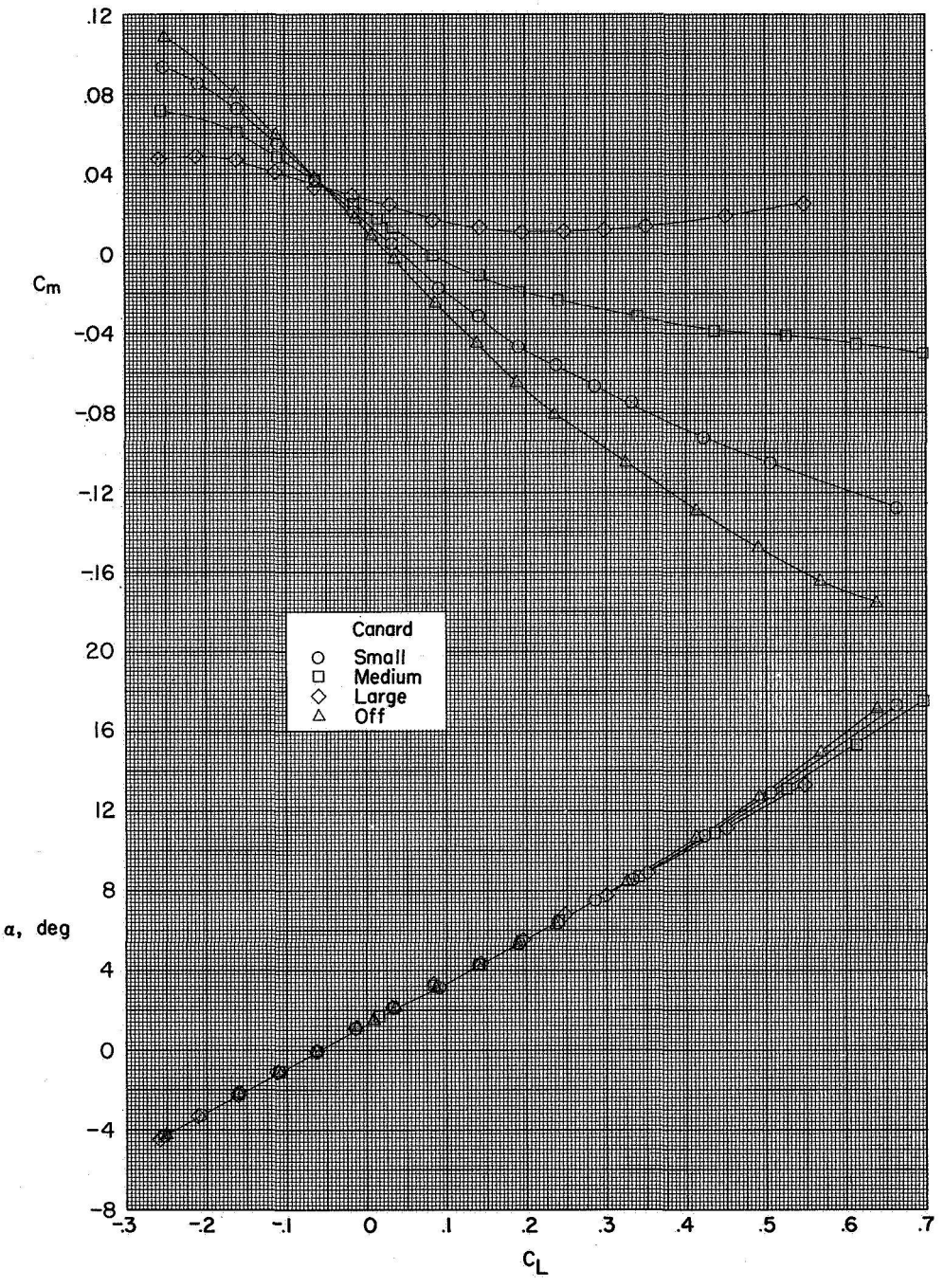

(a) C_m and α against C_L.

Figure 4.- Effect of canard size on aerodynamic characteristics in pitch, for twisted wing, vertical-tail on, swept-wing model. M = 1.41. Center-of-gravity position at body station 21.97.

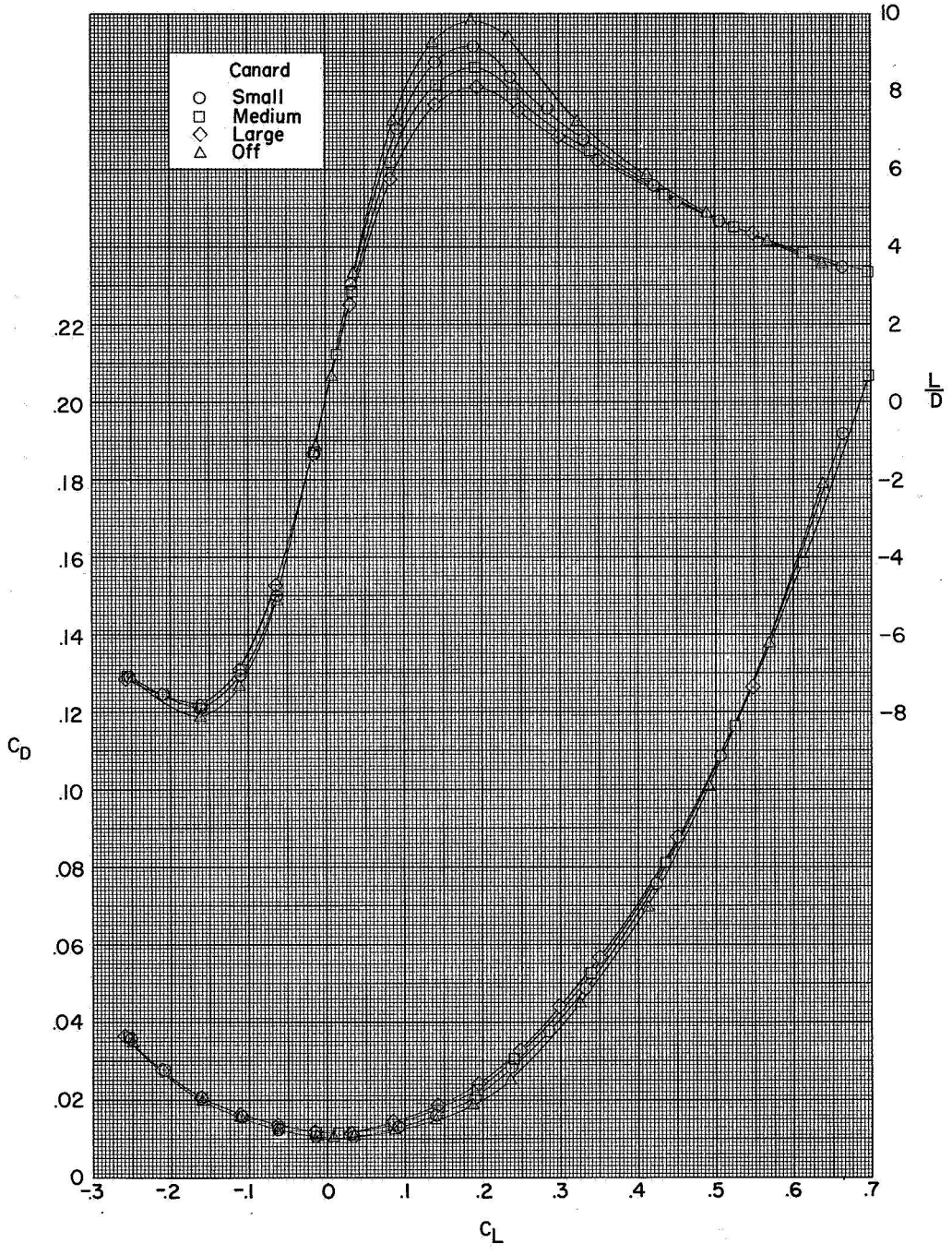

(b) L/D and C_D against C_L.

Figure 4.- Concluded.

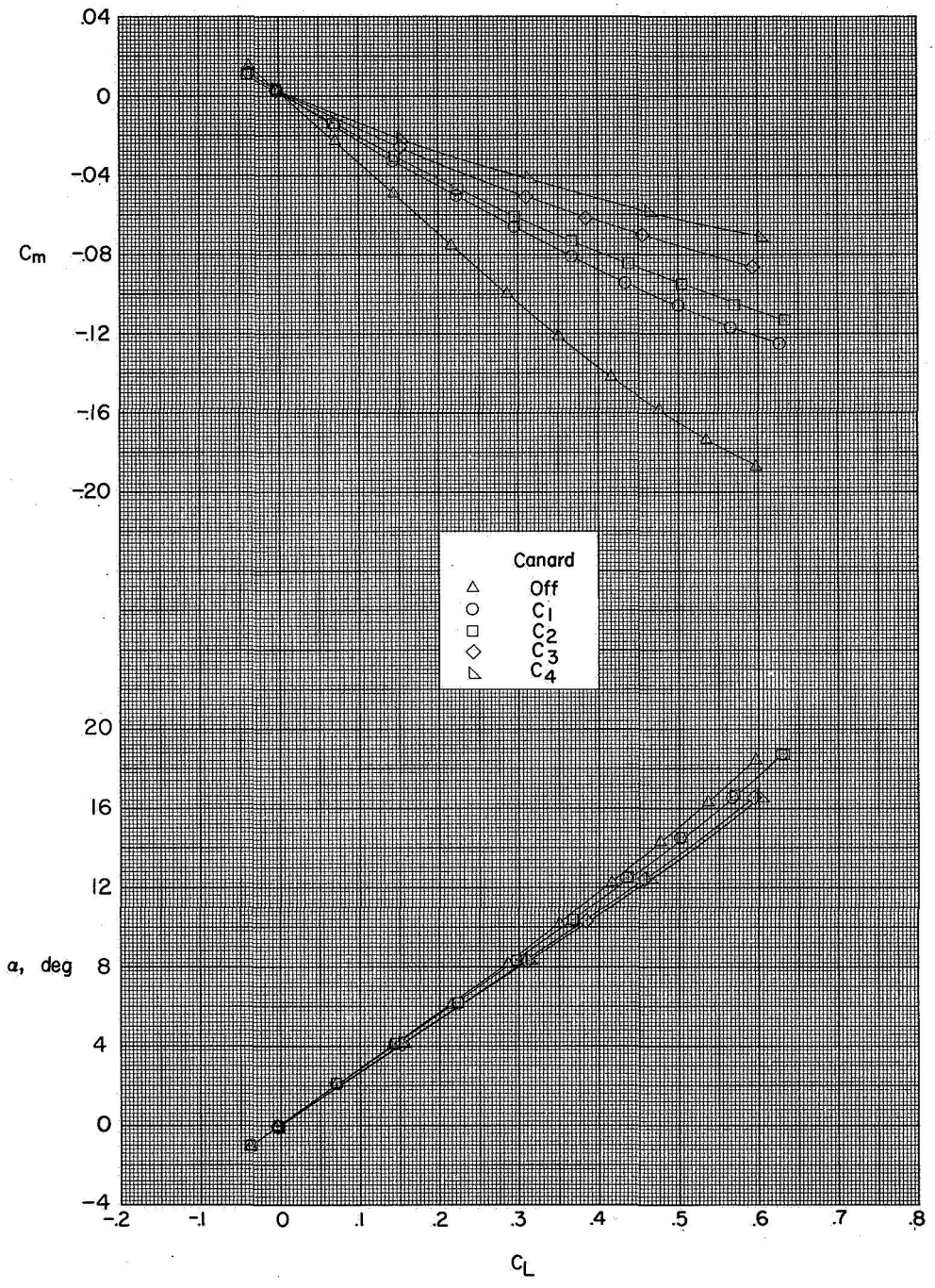

(a) C_m and α against C_L.

Figure 5.- Effect of canard size on aerodynamic characteristics in pitch for 60° delta-midwing configuration. M = 2.01. Center-of-gravity position at body station 25.

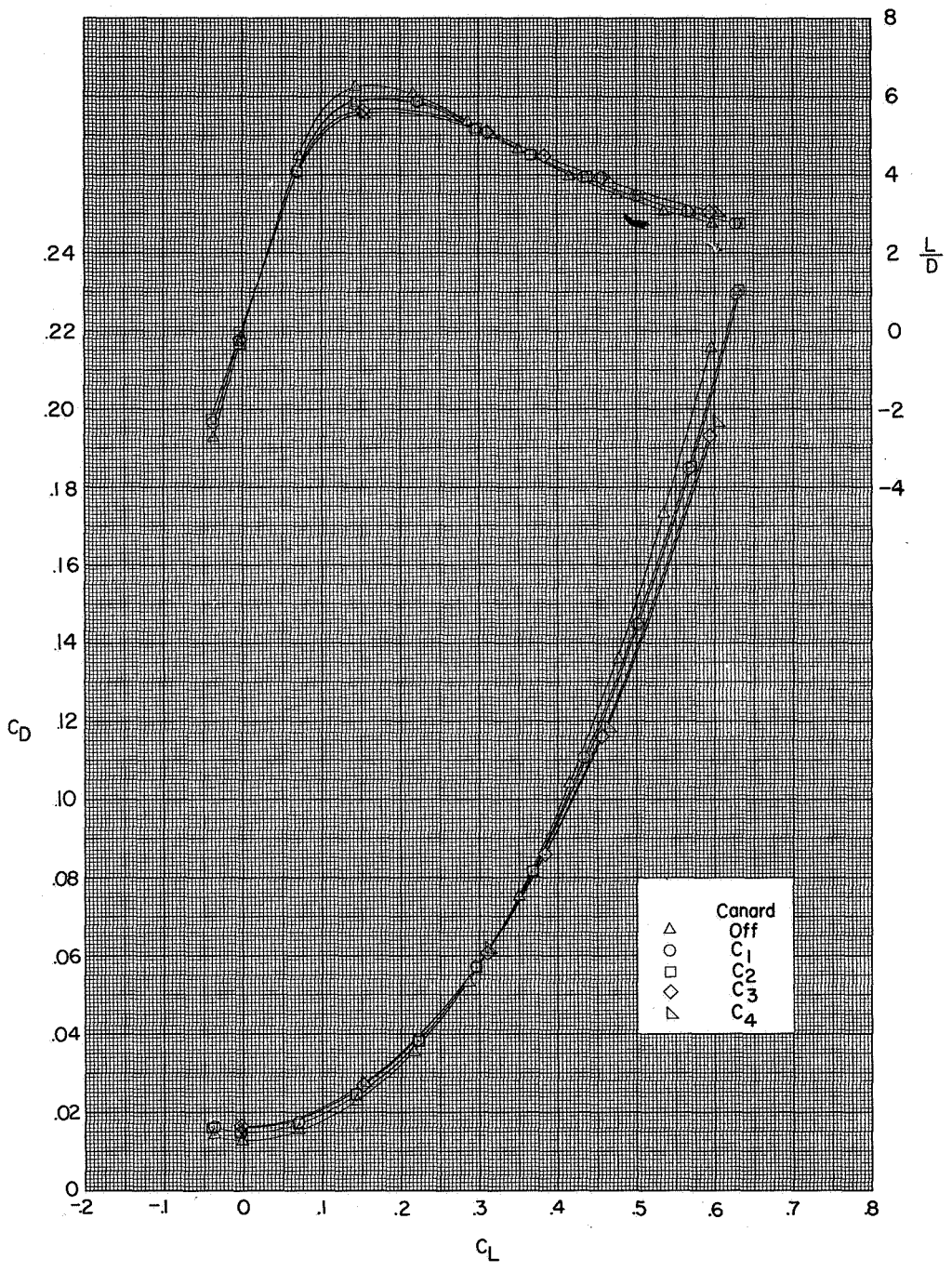

(b) C_D and L/D against C_L.

Figure 5.- Concluded.

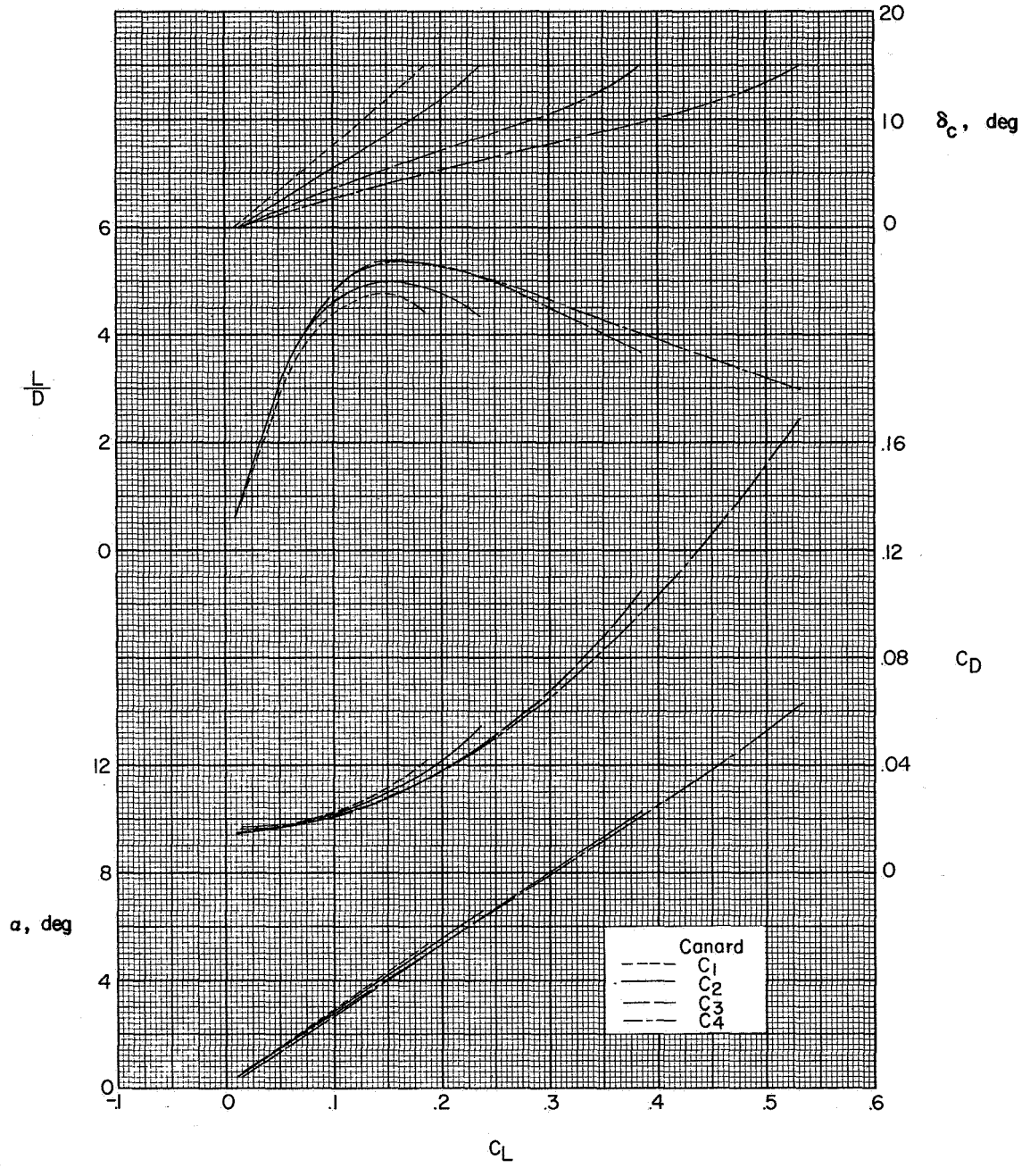

Figure 6.- Effect of canard size on trim longitudinal characteristics for 60° delta-wing $B_1W_2V_5U_1$ configuration. M = 2.01. Center-of-gravity position at body station 25.

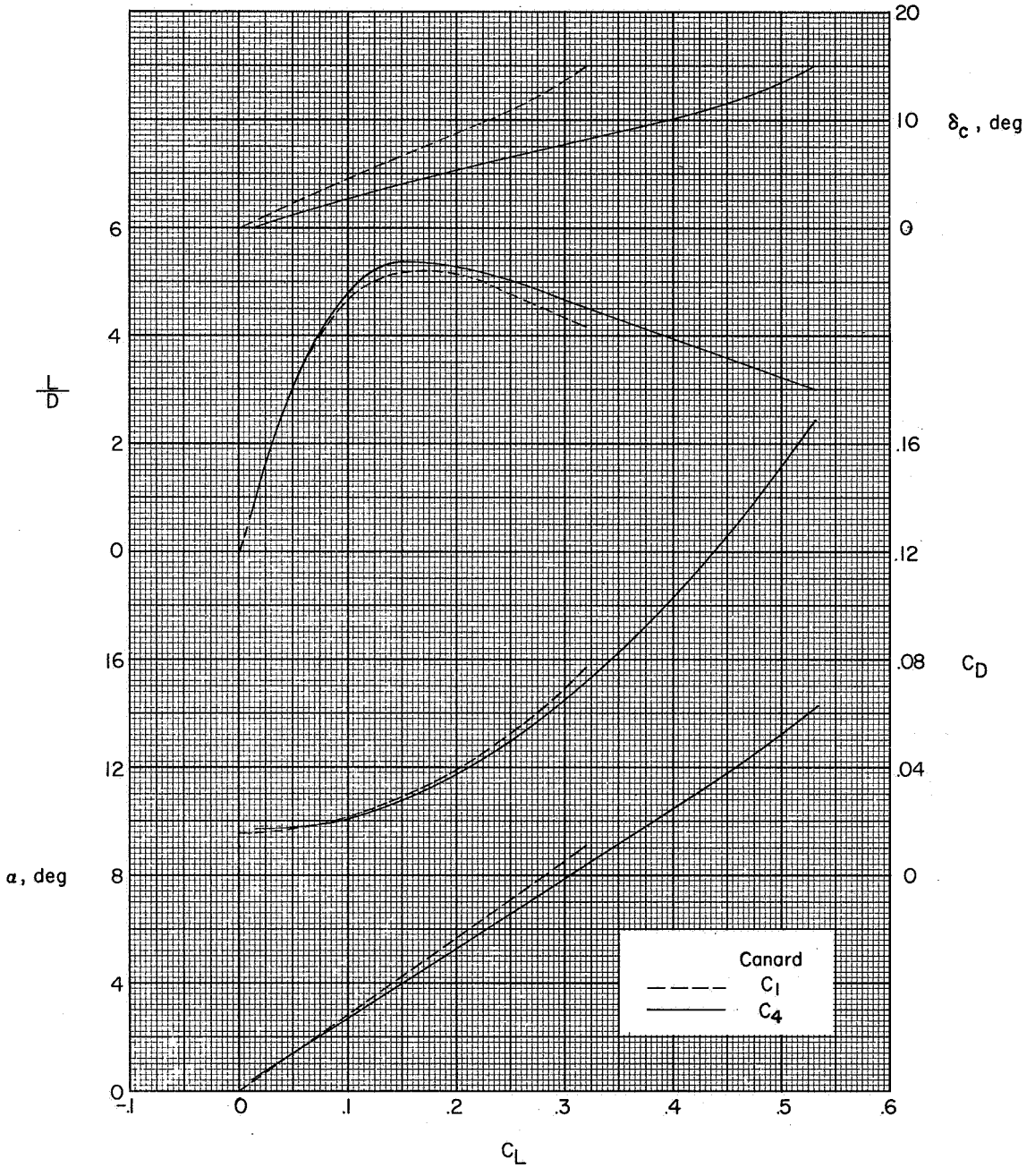

Figure 7.- Effect of canard size on trim longitudinal characteristics for 60° delta-wing $B_1W_2V_5U_1$ configuration. M = 2.01; $\partial C_m/\partial C_L = -0.156$.

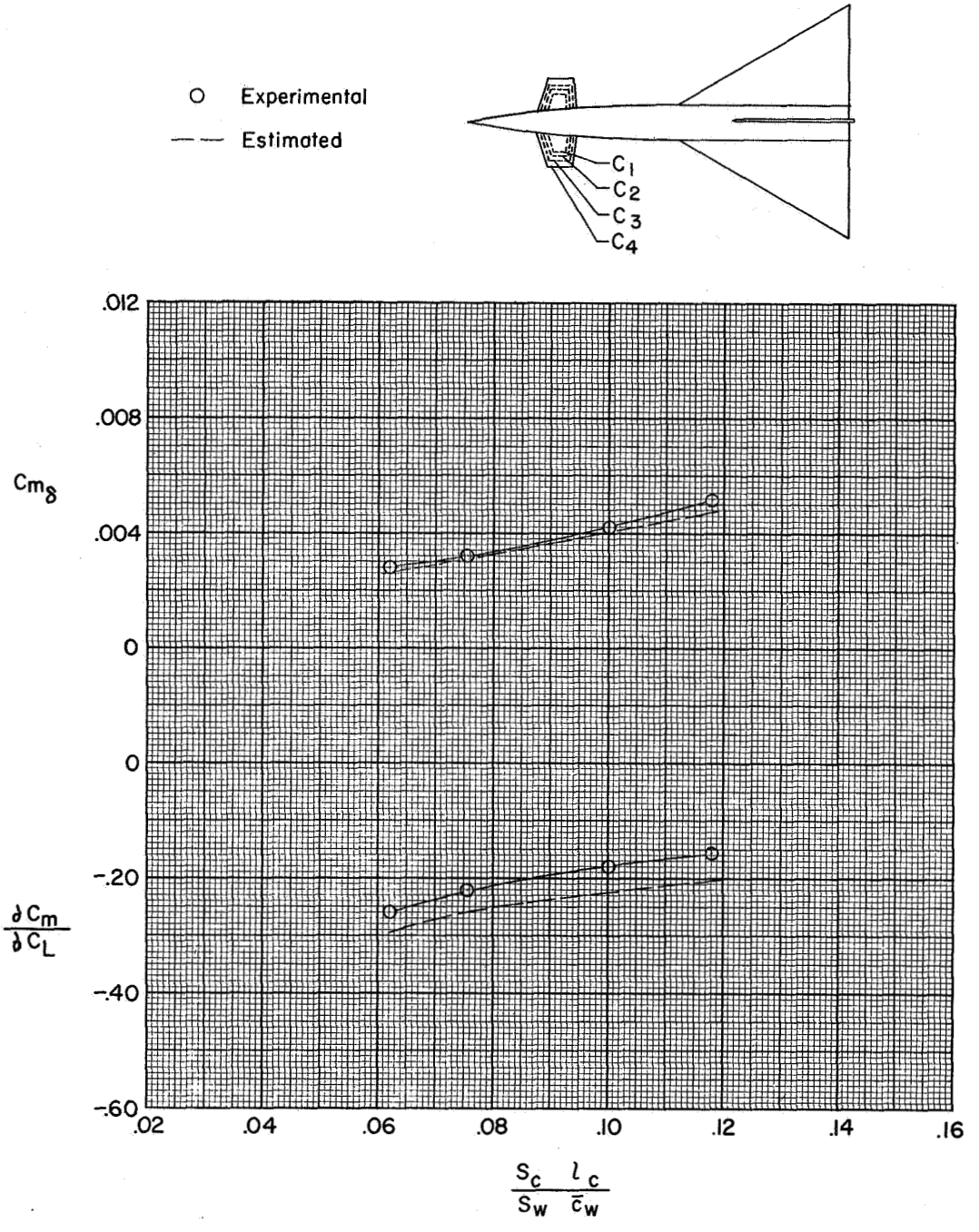

Figure 8.- Variation of canard-control pitch effectiveness and static longitudinal stability with canard volume coefficient for $B_1W_2V_5U_1$ configuration. M = 2.01. Center-of-gravity position at body station 25.

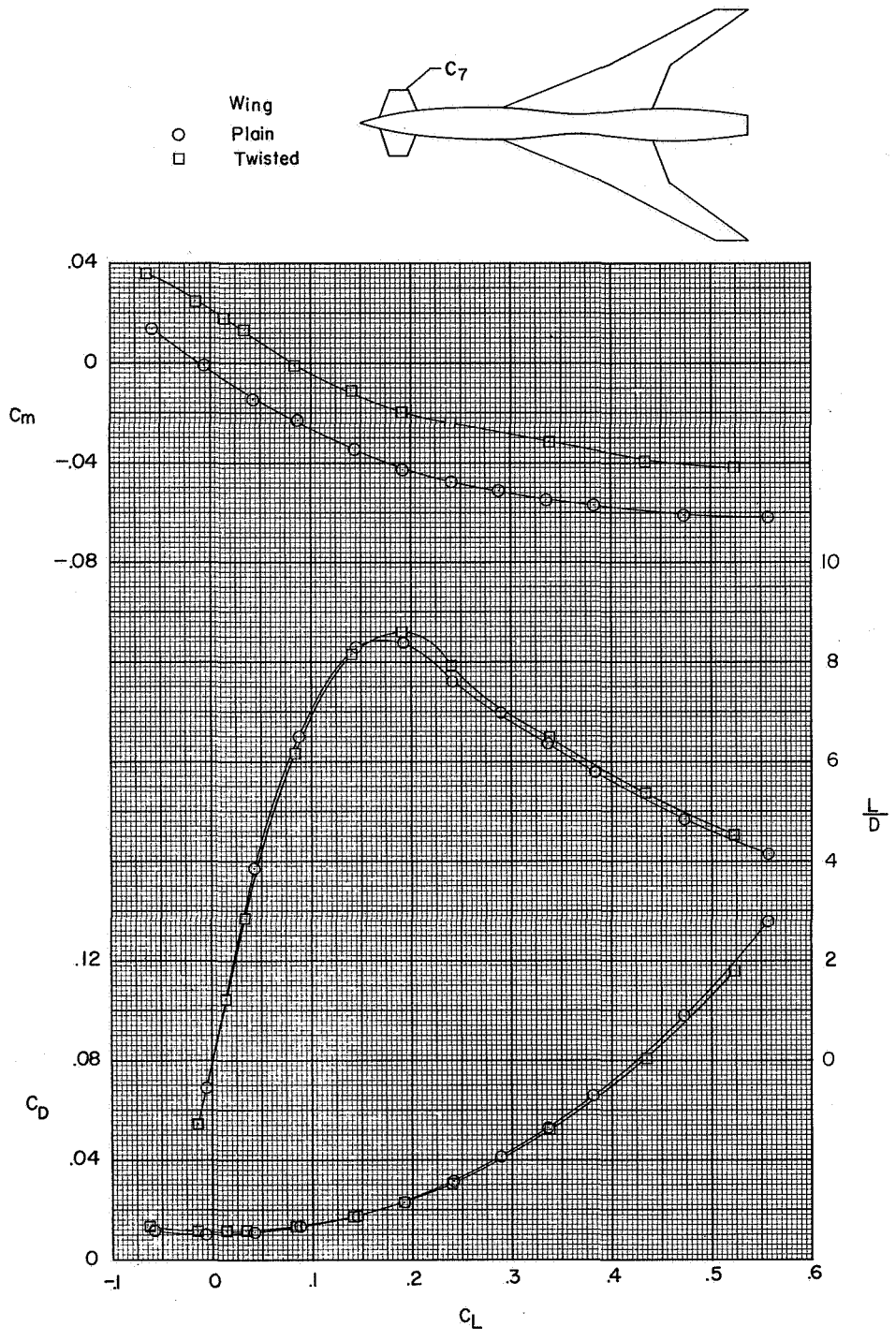

Figure 9.- Effect of wing twist on longitudinal aerodynamic characteristics for swept-wing configuration. M = 1.41. Center-of-gravity position at body station 21.97.

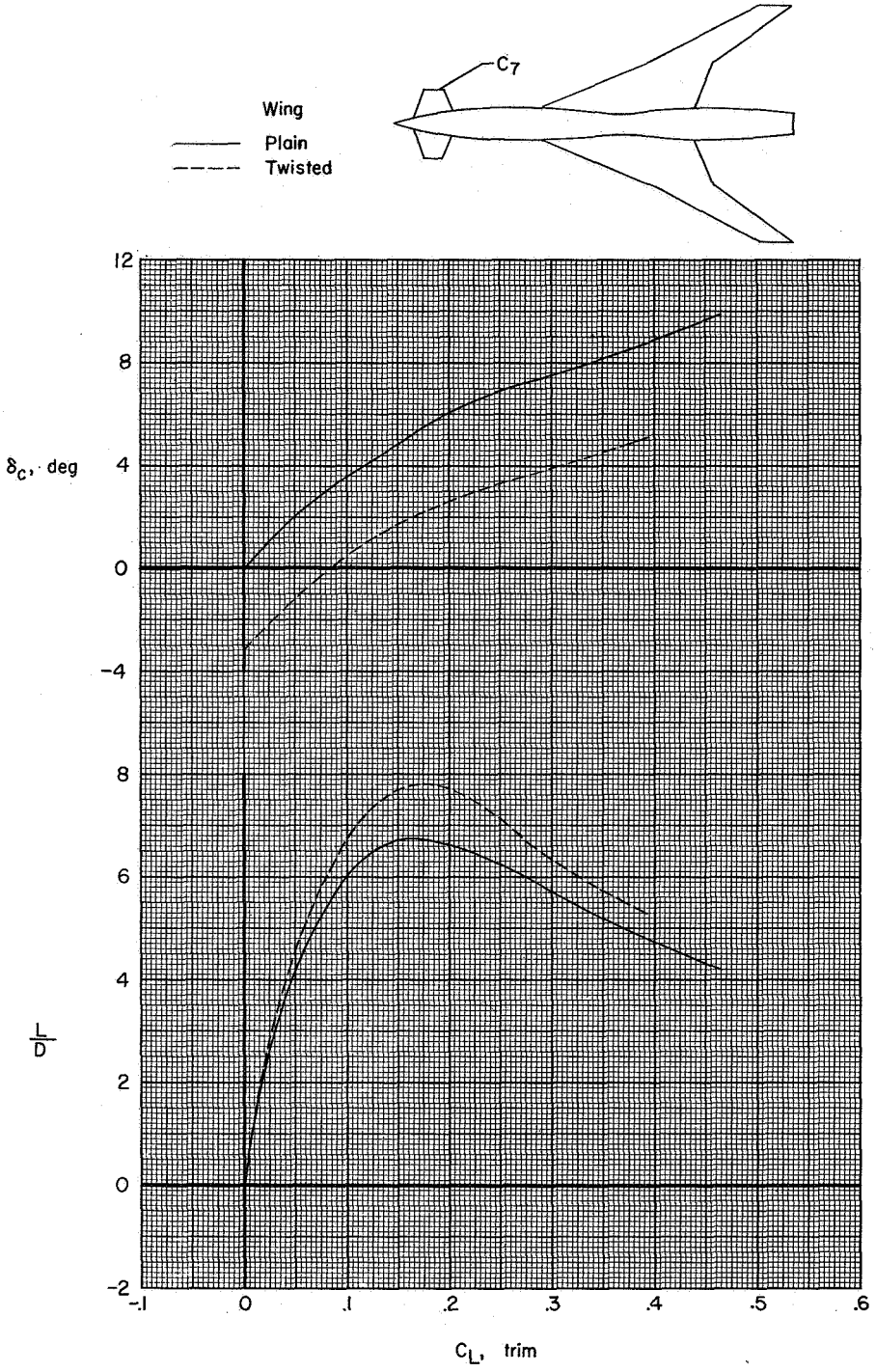

Figure 10.- Effect of wing twist on trim longitudinal characteristics for swept-wing configuration. M = 1.41; $\partial C_m / \partial C_L$ = -0.24.

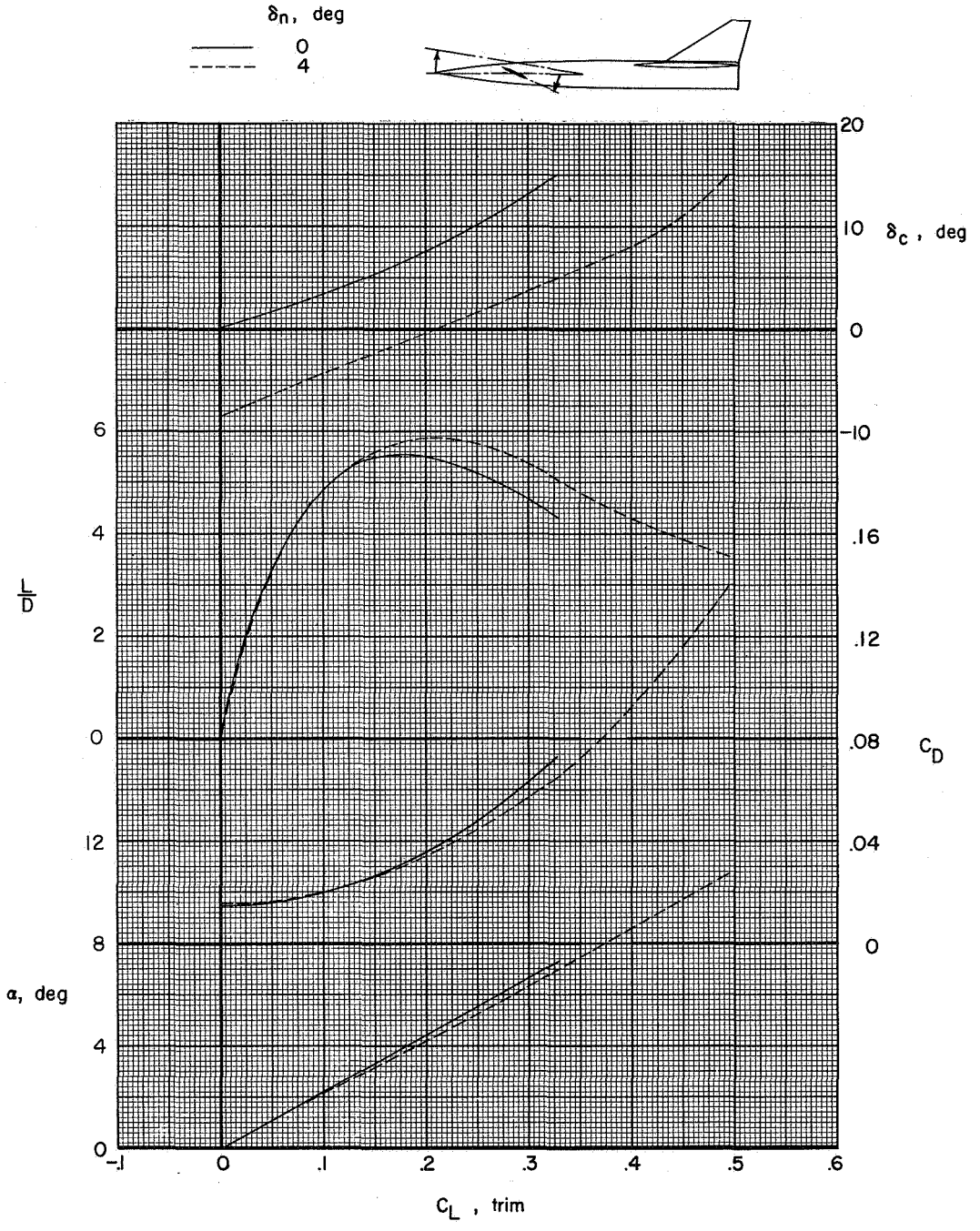

Figure 11.- Effect of forebody deflection on trim longitudinal characteristics for trapezoidal high-wing $B_4W_3V_2C_2$ configuration. M = 2.01; $\partial C_m / \partial C_L = -0.24$.

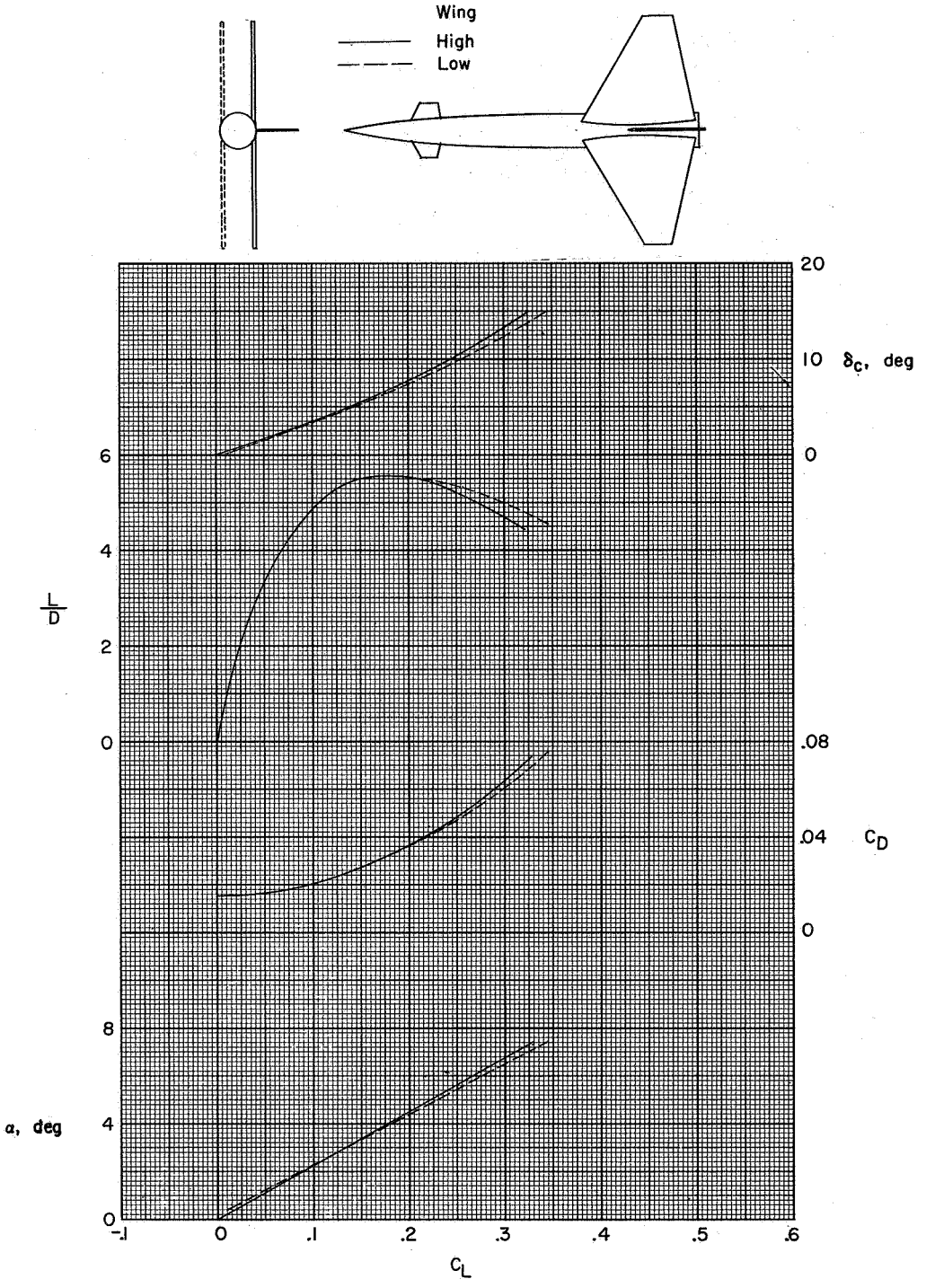

Figure 12.- Effect of wing vertical location on trim longitudinal characteristics for $B_4W_3V_2C_2$ configuration. M = 2.01; $\partial C_m/\partial C_L$ = -0.244.

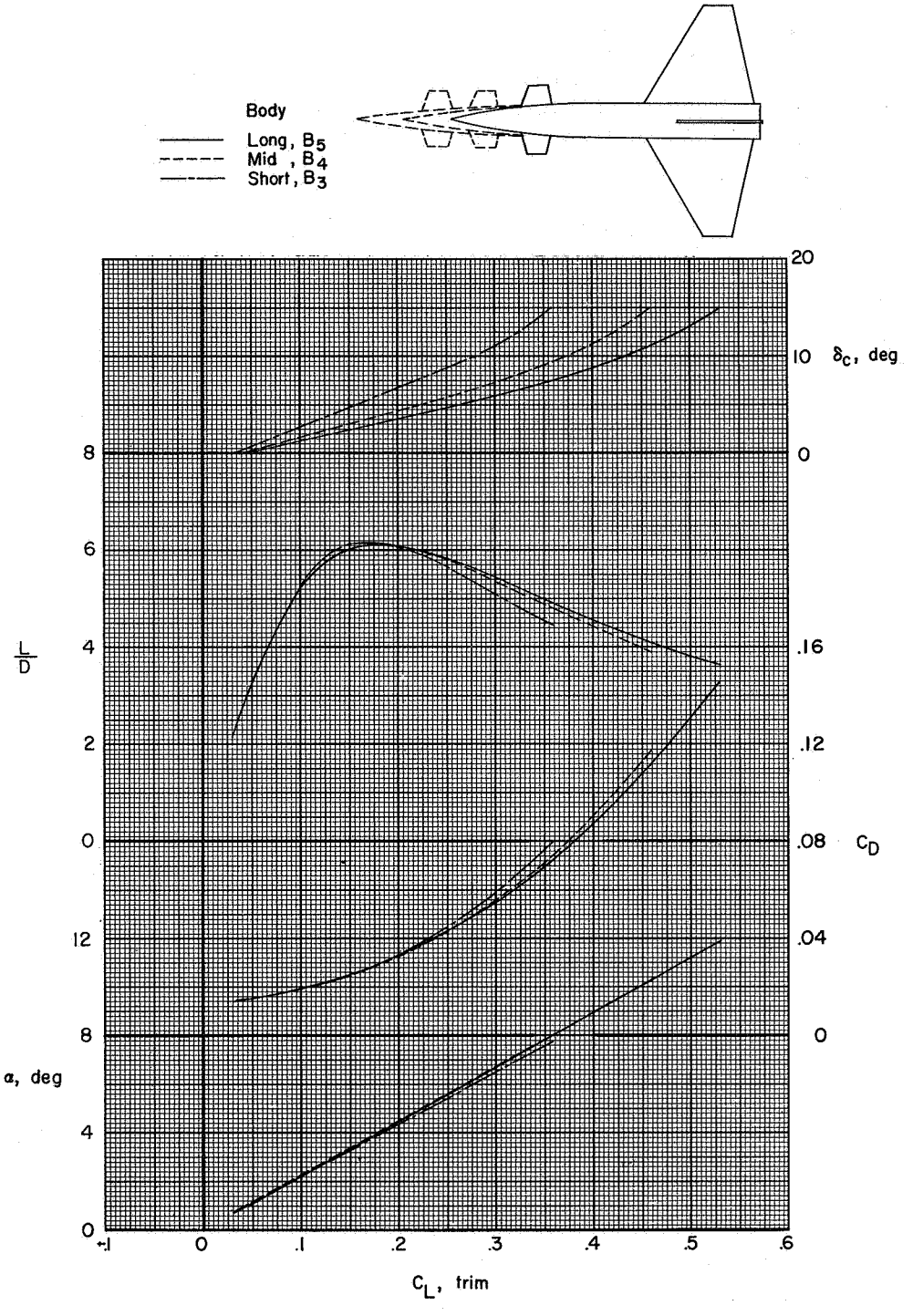

Figure 13.- Effect of body length on trim longitudinal characteristics for midwing $W_3V_2C_2$ configuration. $M = 2.01$; $\partial C_m/\partial C_L = -0.172$.

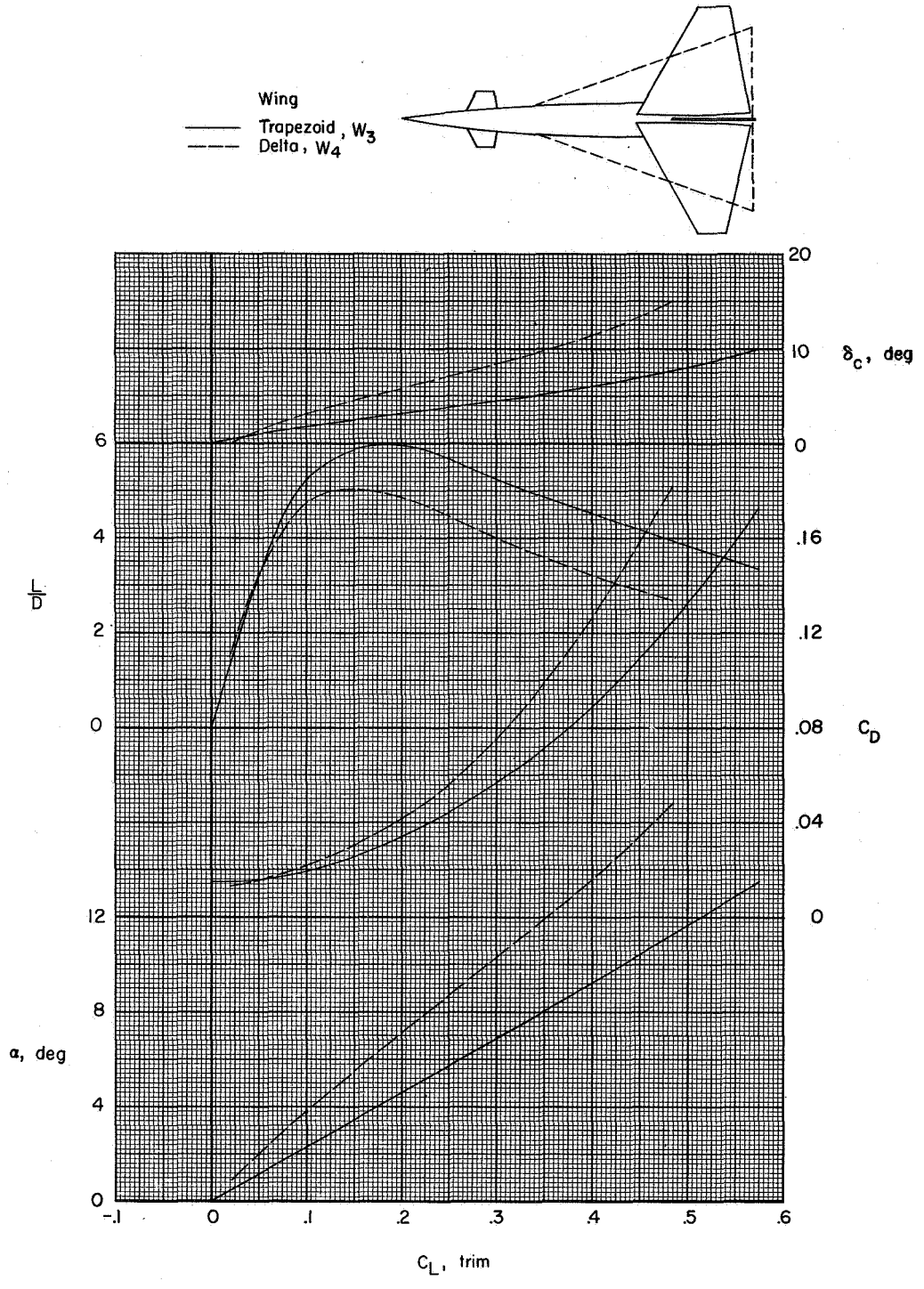

Figure 14.- Effect of wing plan form on trim longitudinal characteristics for $B_4V_2C_2$ high-wing configuration. M = 2.01; $\partial C_m/\partial C_L = -0.10$.

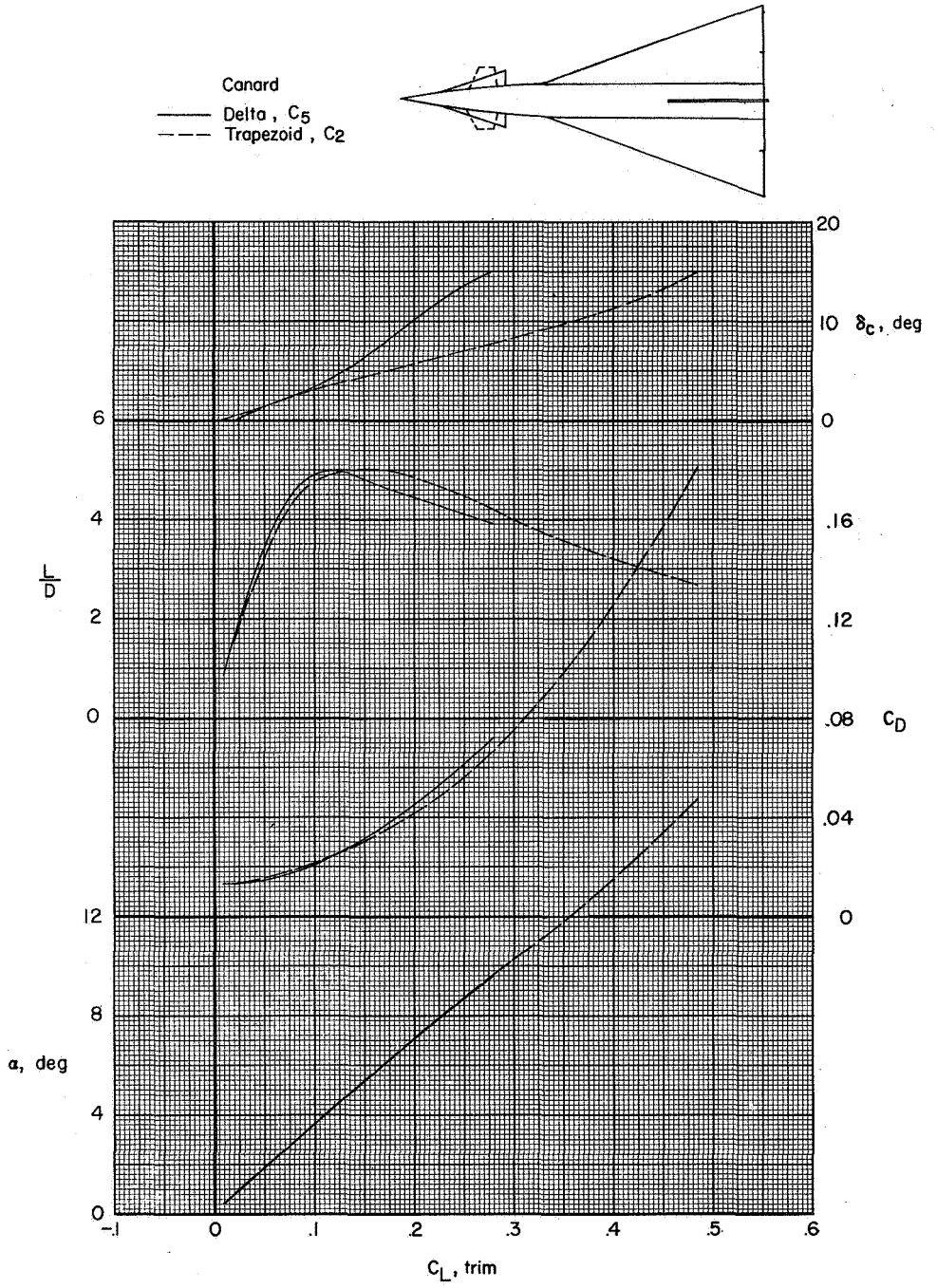

Figure 15.- Effect of canard-surface plan form on trim longitudinal characteristics for $B_4W_4V_2$ midwing configuration. M = 2.01; $\partial C_m/\partial C_L$ = -0.10.

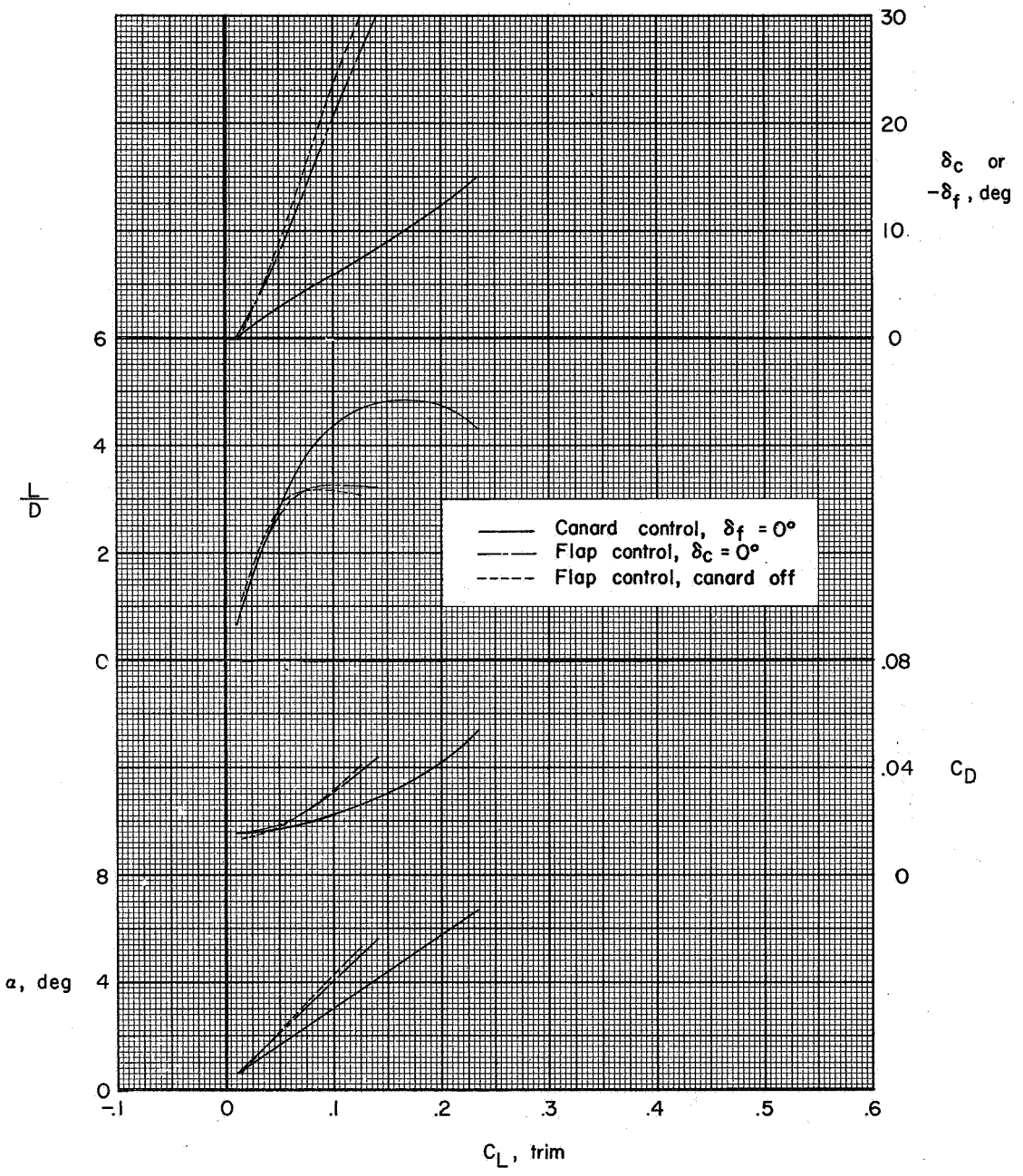

Figure 16.- Comparison of longitudinal trim characteristics with canard control and trailing-edge flap control for $B_1W_2V_4C_2$ configuration. M = 2.01; $\partial C_m / \partial C_L = -0.22$.

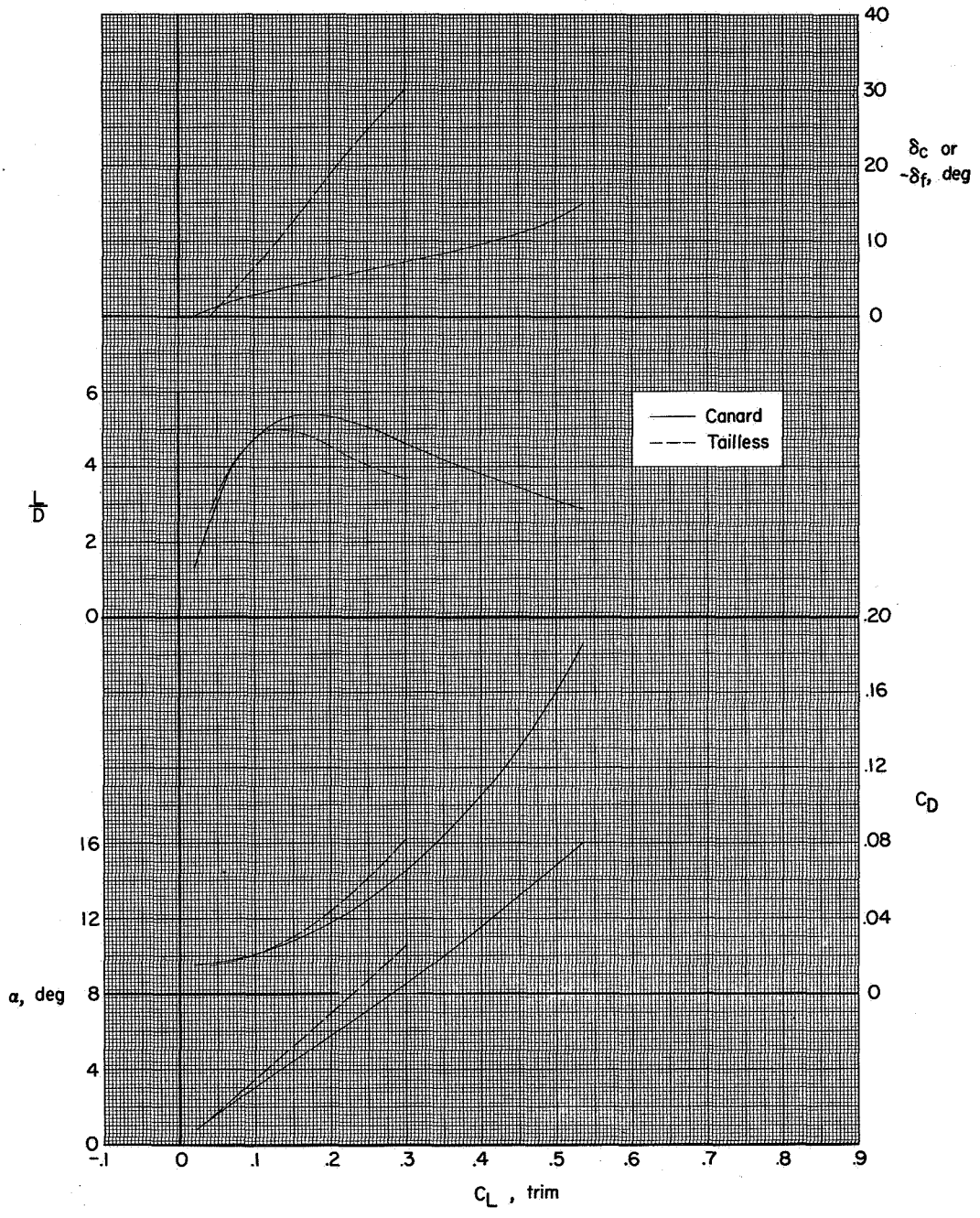

Figure 17.- Comparison of longitudinal trim characteristics with canard control and trailing-edge flap control for $B_1W_2V_4$ configuration with C_2 on and off. M = 2.01; $\partial C_m/\partial C_L$ = -0.10.

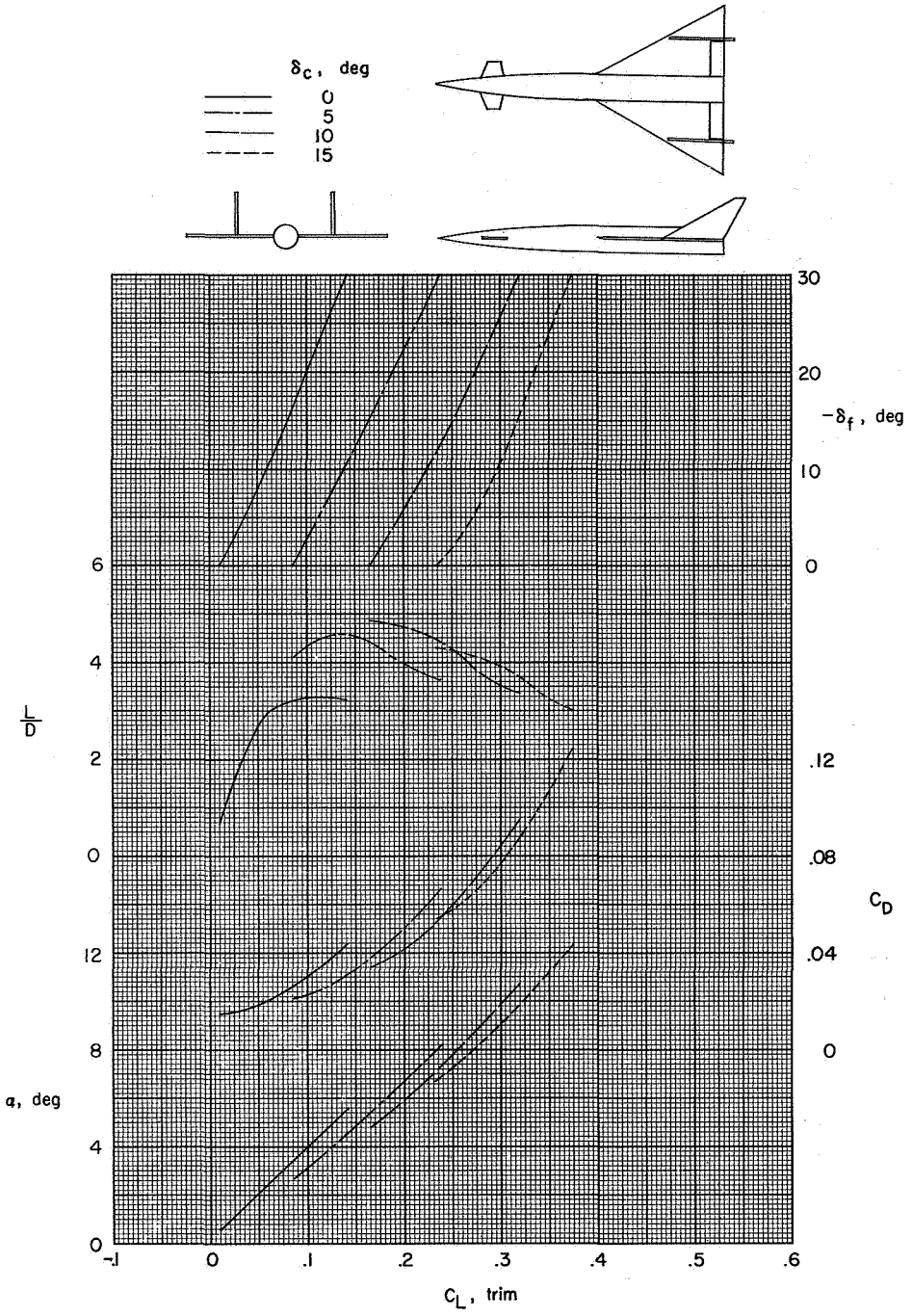

Figure 18.- Effect of canard deflection on trim longitudinal characteristics for configuration with trailing-edge flap controls for $B_1W_2V_4C_2$ configuration. M = 2.01; $\partial C_m/\partial C_L$ = -0.22.

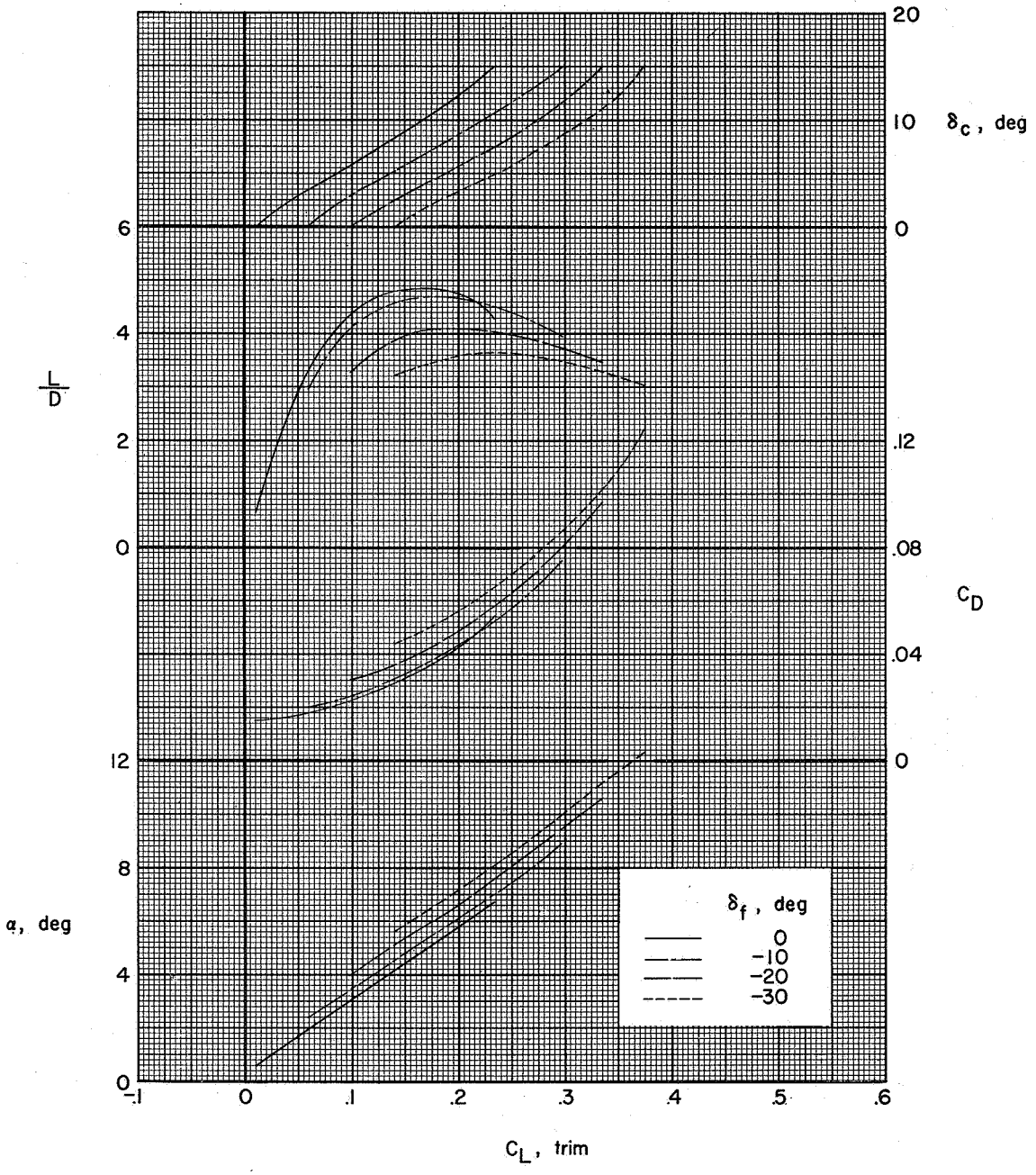

Figure 19.- Effect of canard deflection on longitudinal trim characteristics with various trailing-edge flap deflections for $B_1W_2V_4C_2$ configuration. $M = 2.01$; $\partial C_m/\partial C_L = -0.22$.

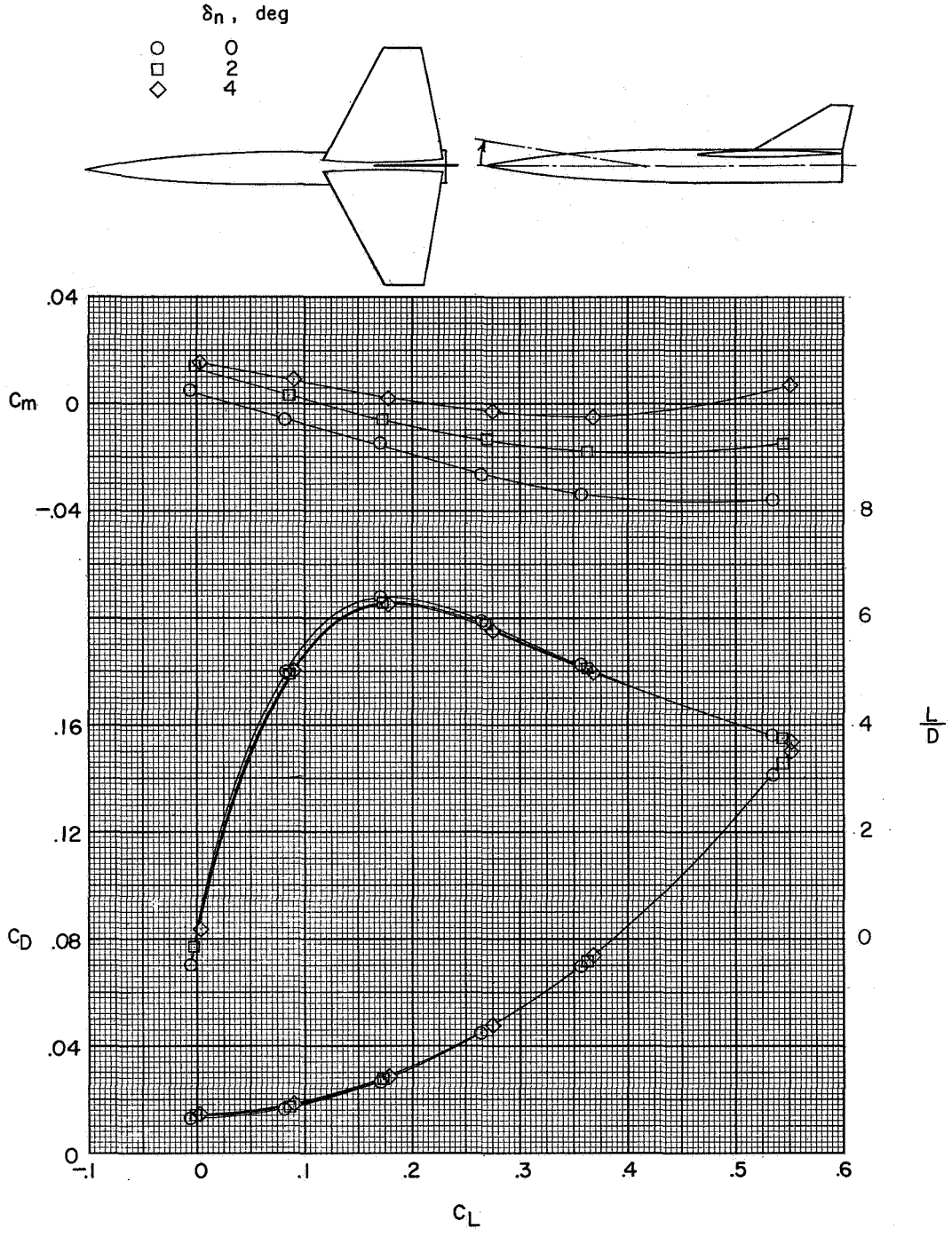

Figure 20.- Effect of forebody deflection on longitudinal aerodynamic characteristics for trapezoidal high-wing $B_4W_3V_2$ configuration.

M = 2.01. Center-of-gravity position at body station 28.13.

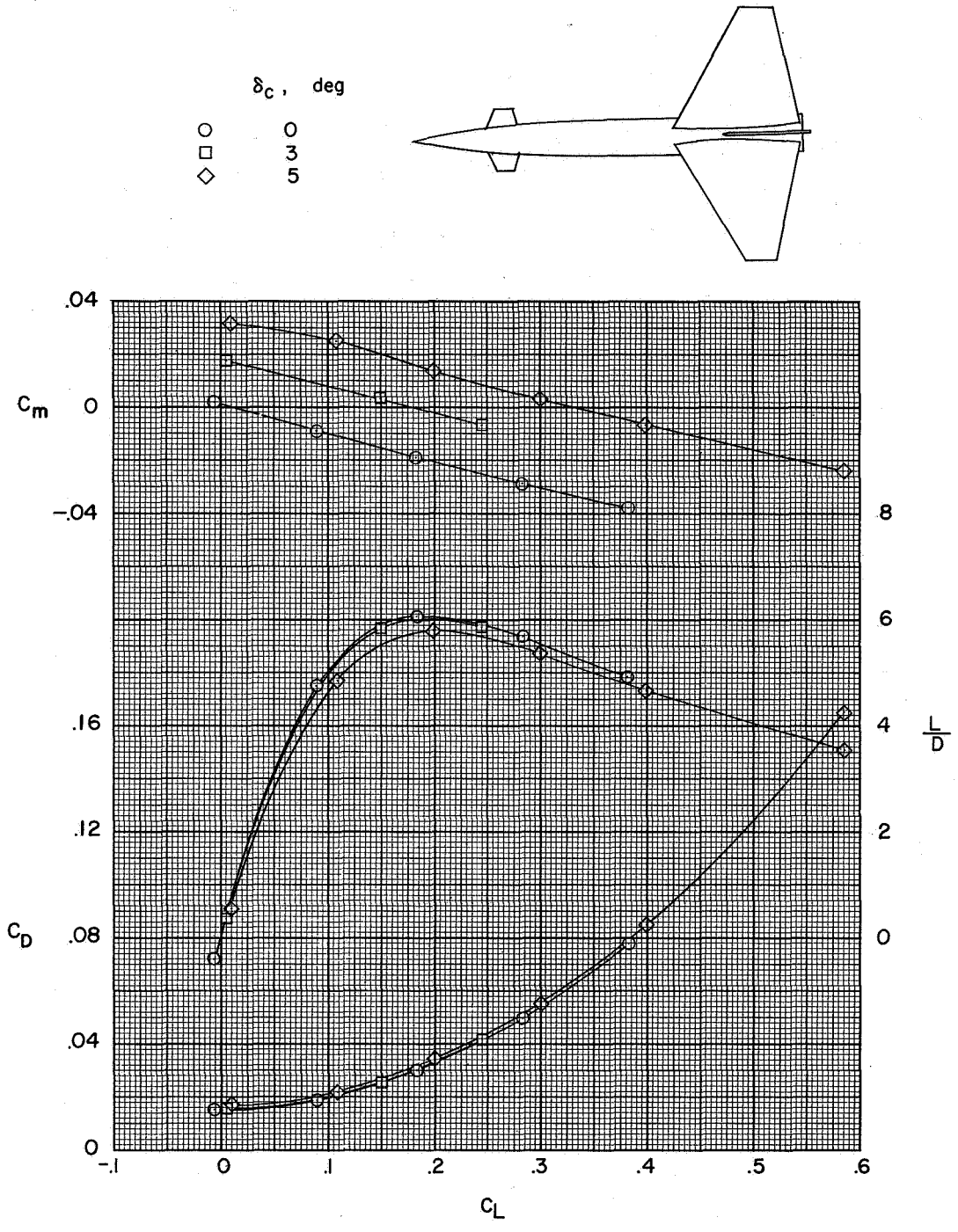

Figure 21.- Effect of canard deflection on longitudinal aerodynamic characteristics for trapezoidal high-wing $B_4W_3V_2C_2$ configuration. M = 2.01. Center-of-gravity position at body station 26.17.

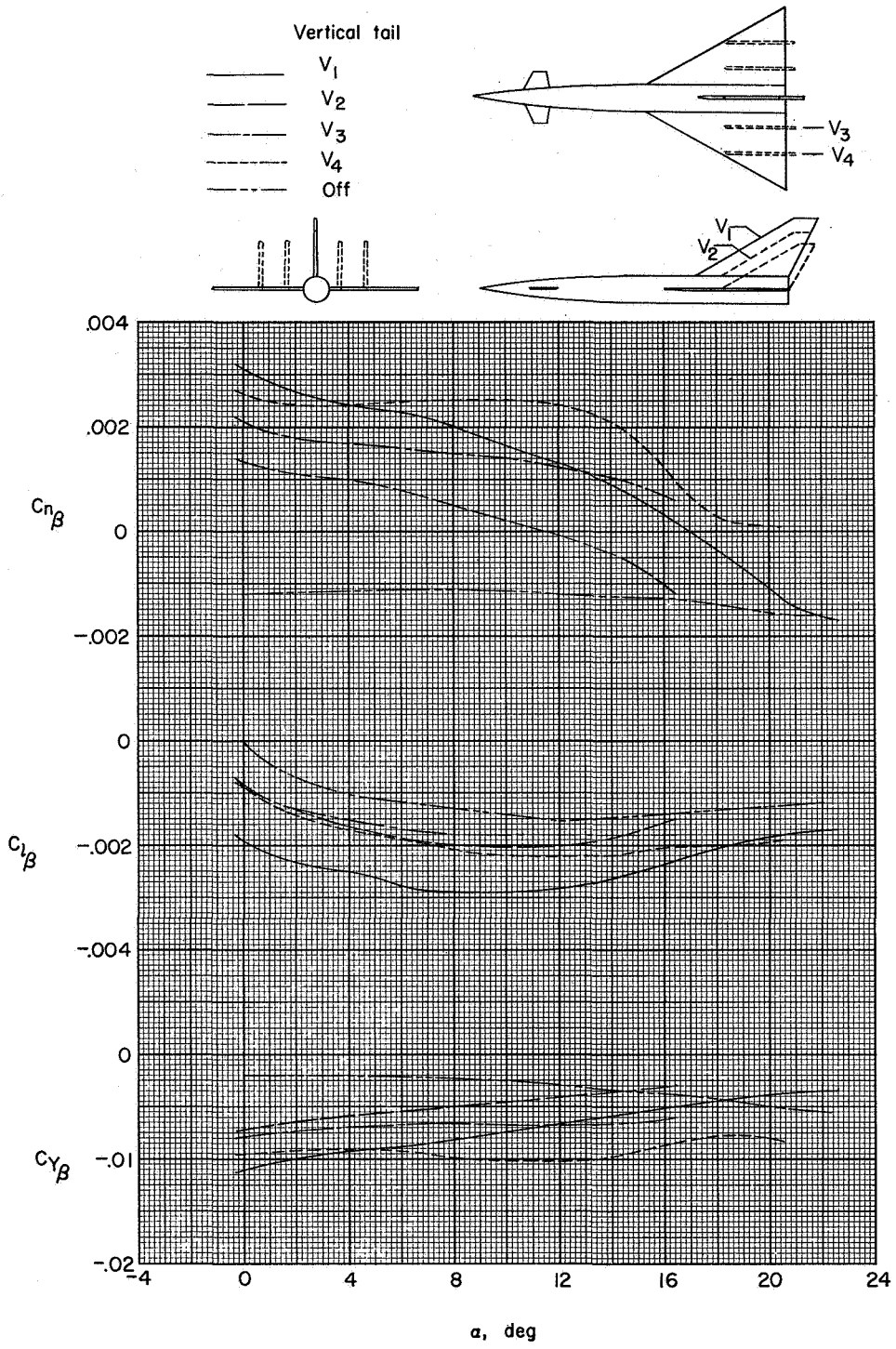

Figure 22.- Effect of vertical-tail arrangement on sideslip derivatives for 60° delta midwing $B_1W_2C_2$ configuration. M = 2.01; δ_c = 0°.

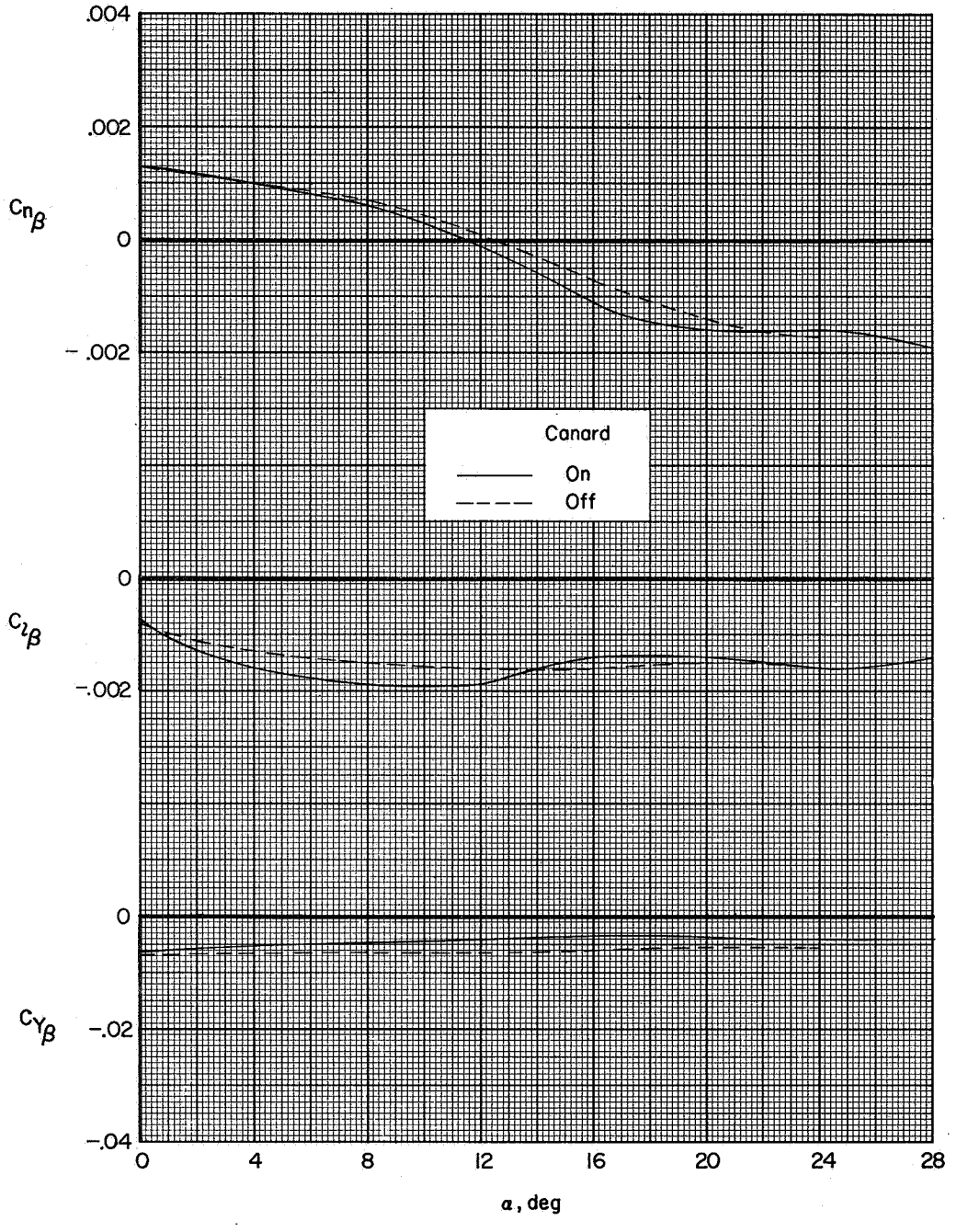

(a) Single vertical tail, V_2.

Figure 23.- Effect of canard surface on sideslip derivatives for model with single and twin vertical tails. $B_1W_2C_2$ configuration. M = 2.01; $\delta_c = \delta_f = 0^\circ$.

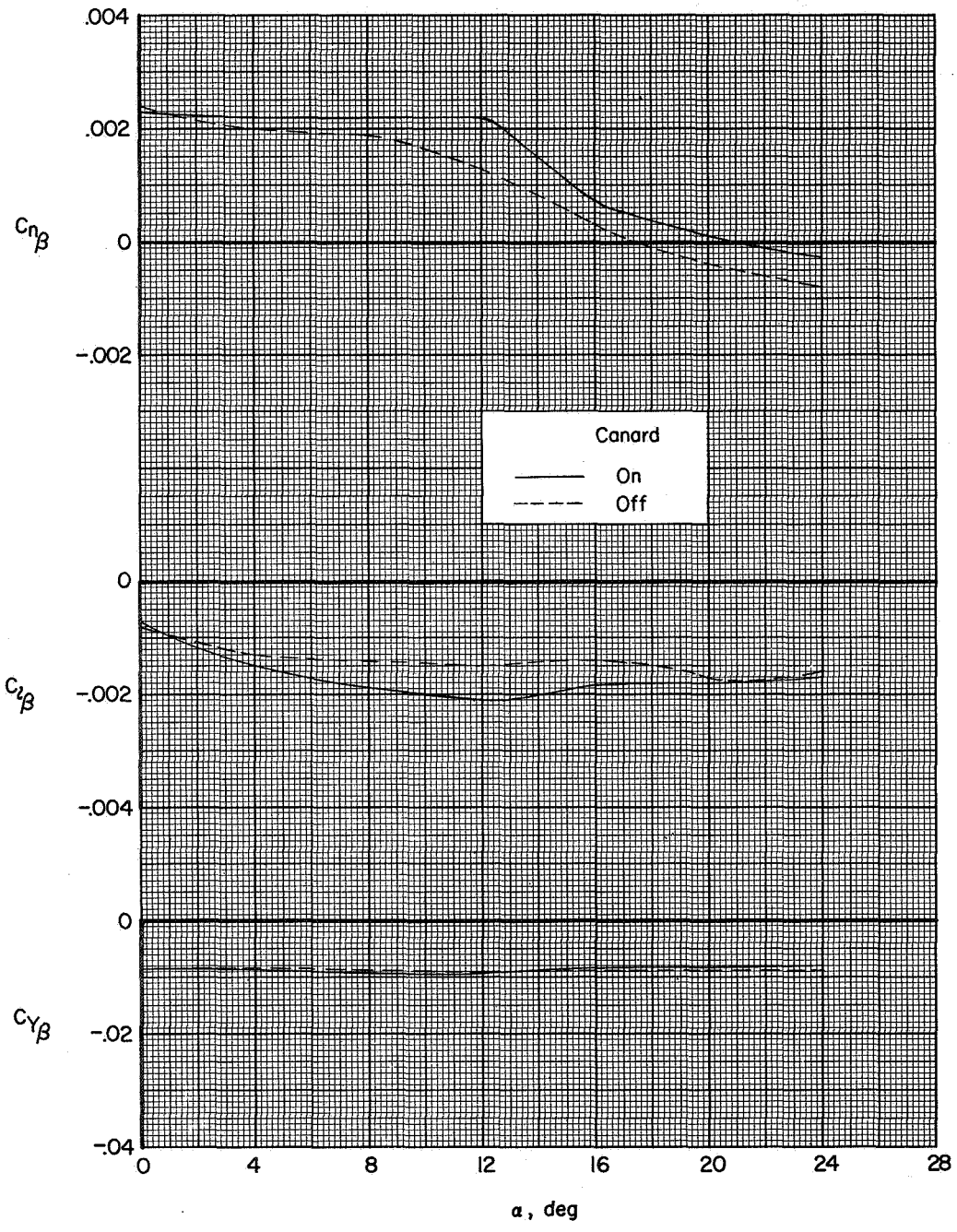

(b) Twin vertical tails, V_4.

Figure 23.- Concluded.

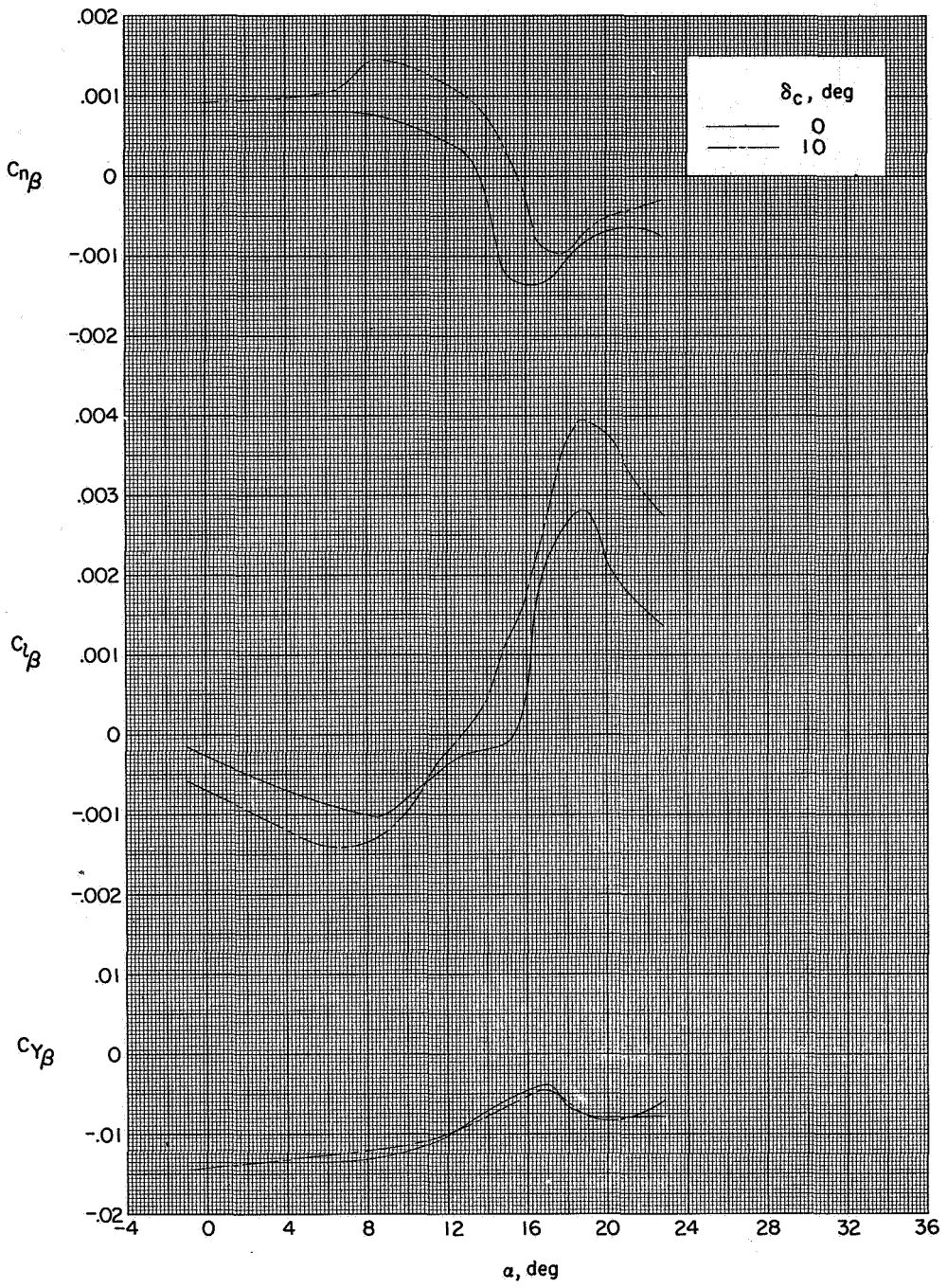

(a) M = 0.60.

Figure 24.- Variation of sideslip derivatives with angle of attack for $B_1W_1V_5C_2U_1$ configuration.

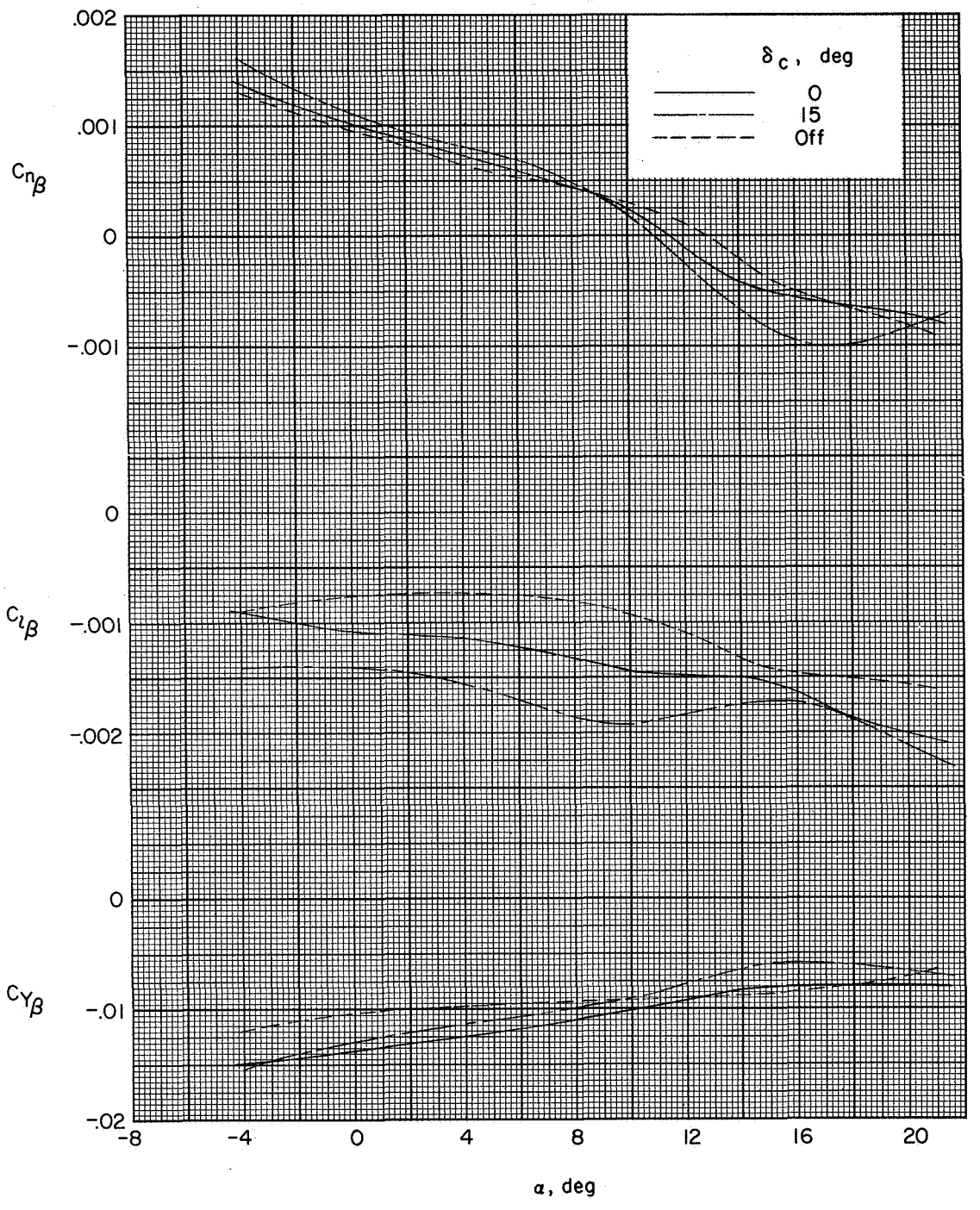

(b) M = 2.29.

Figure 24.- Continued.

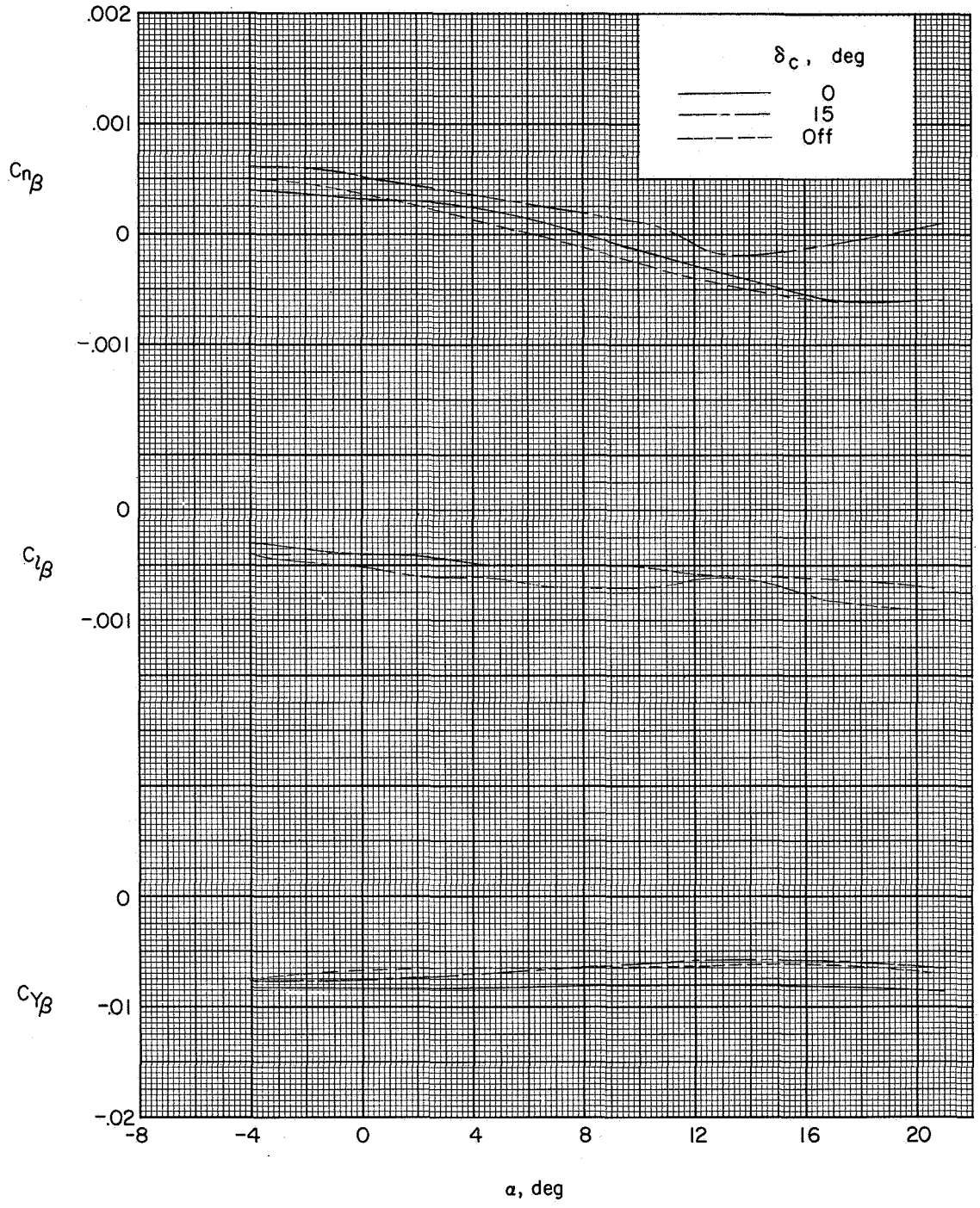

(c) M = 4.65.

Figure 24.- Concluded.

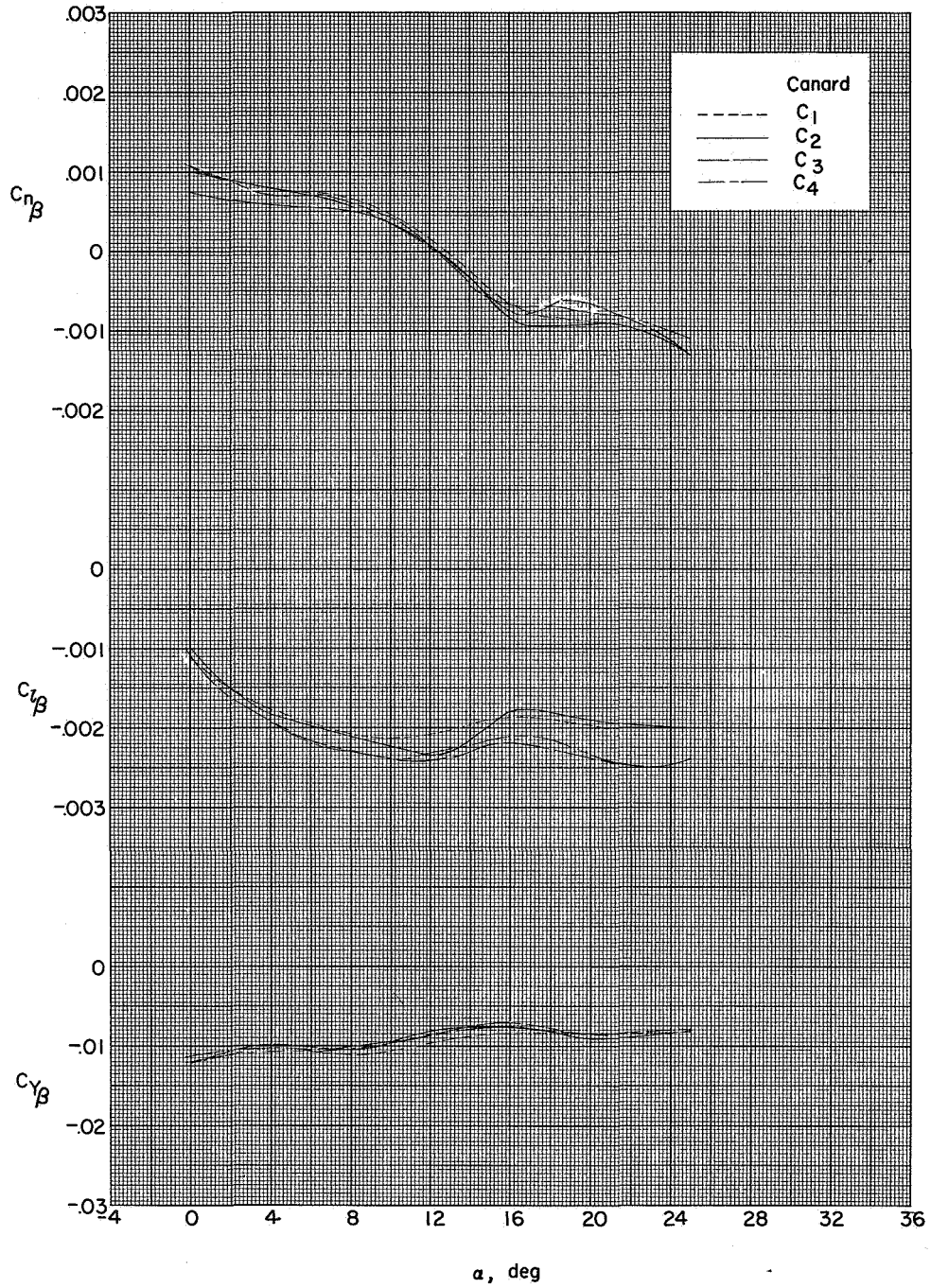

Figure 25.- Effect of canard size on sideslip derivatives for 60° delta-wing $B_1W_2V_5U_1$ configuration. M = 2.01; δ_c = 0°.

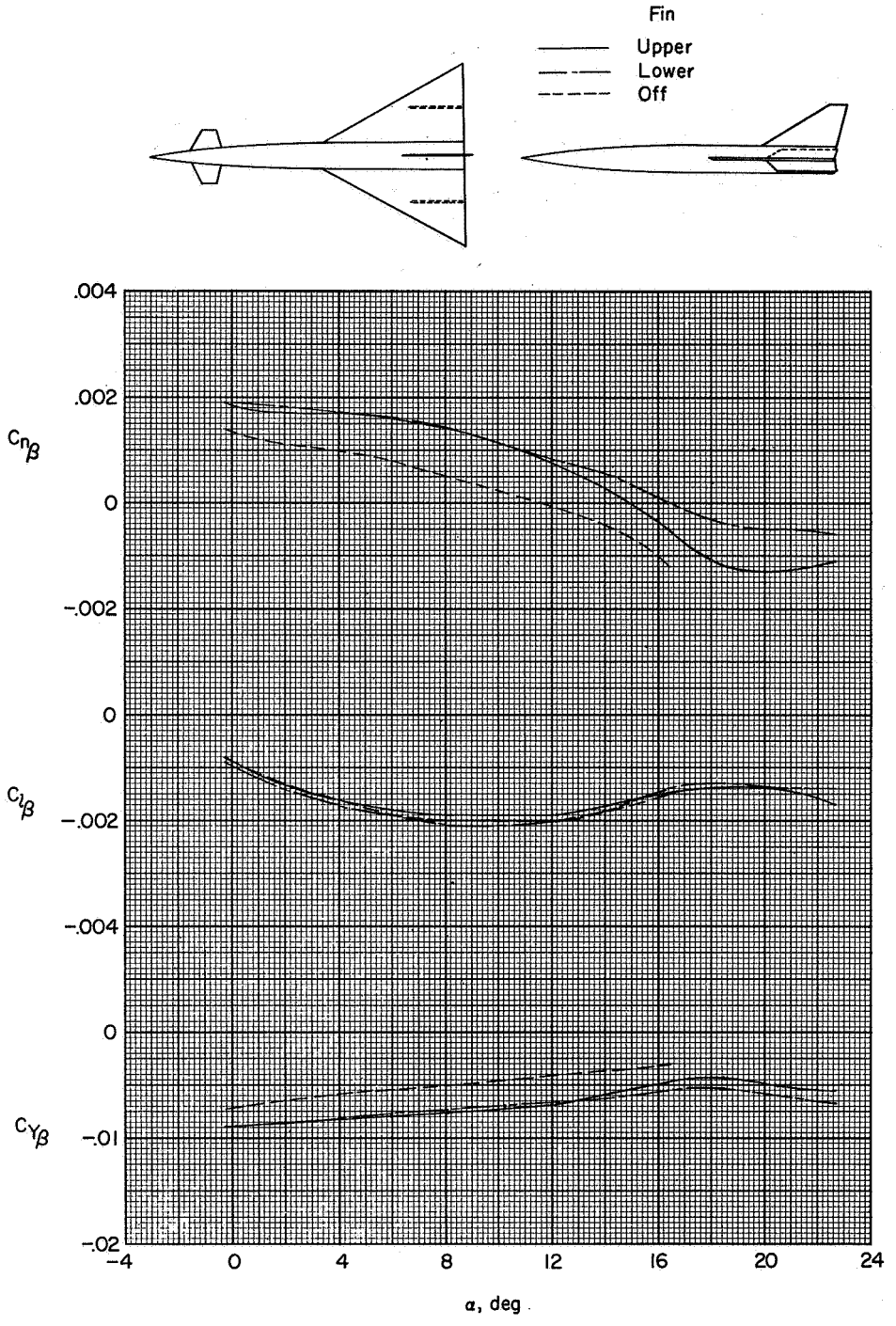

Figure 26.- Effect of wing-mounted fins on sideslip derivative, for 60° delta-midwing $B_1W_2V_2C_2U_3$ configuration with single vertical tail. M = 2.01; $\delta_c = 0°$.

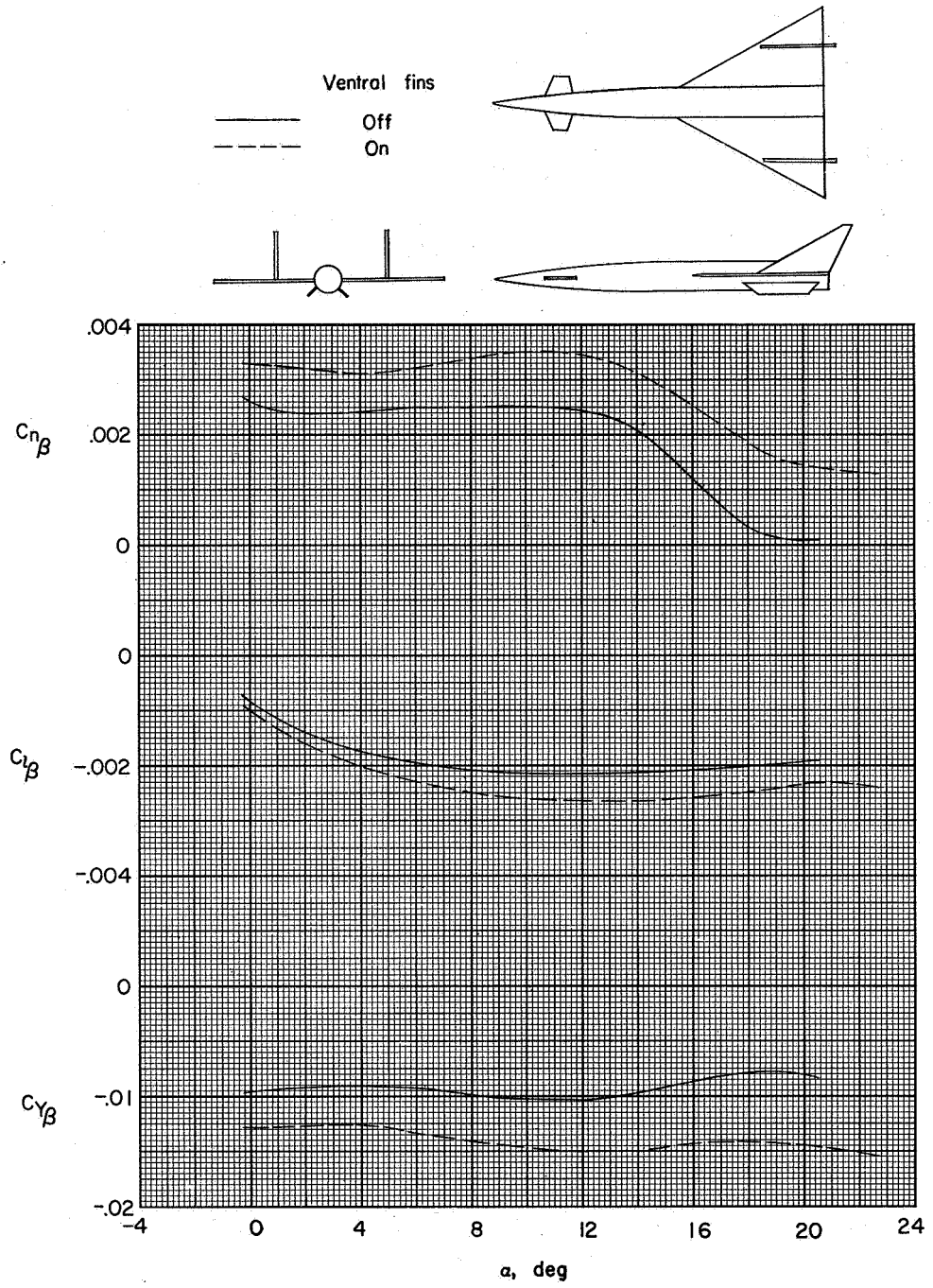

Figure 27.- Effect of body-mounted ventral fins on sideslip derivatives for 60° delta-midwing $B_1W_2V_4C_2U_2$ configuration with twin vertical tails. M = 2.01; δ_c = 0°.

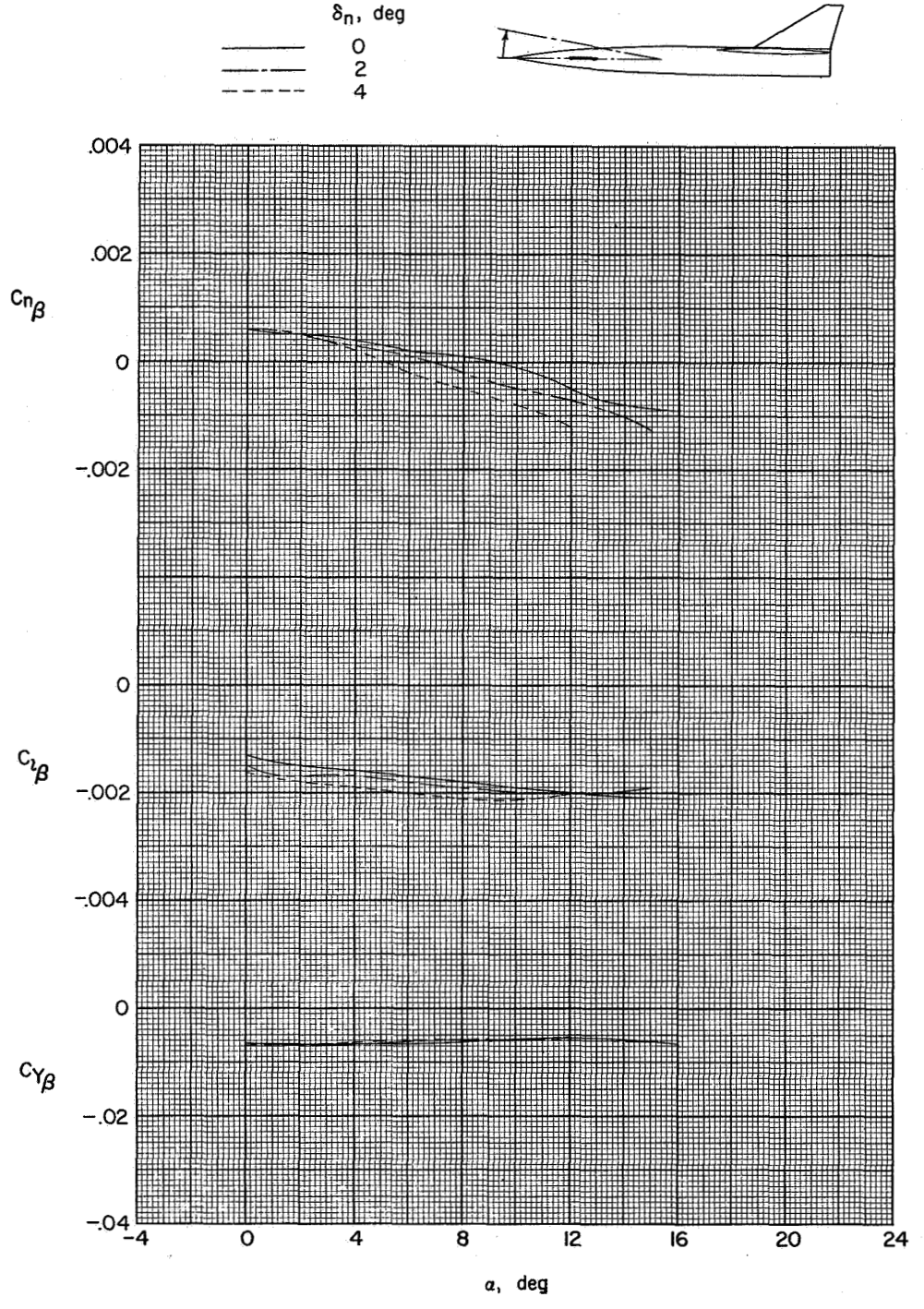

Figure 28.- Effect of forebody deflection on sideslip derivatives for trapezoidal high-wing $B_4W_3V_2C_2$ configuration with single vertical tail. M = 2.01; $\delta_c = 0^o$.

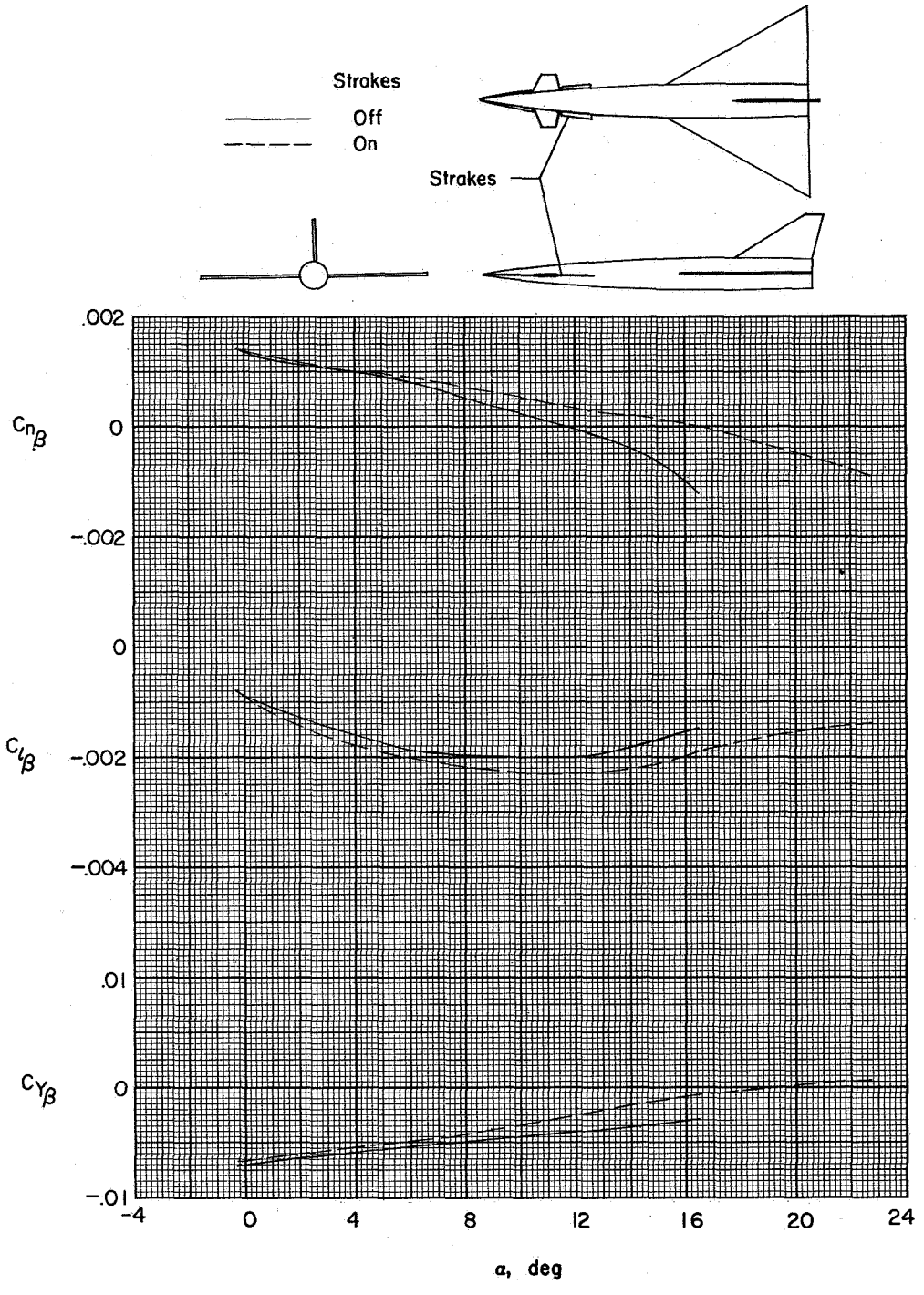

Figure 29.- Effect of forebody strakes on sideslip derivatives for 60° delta-midwing $B_1W_2V_2C_2$ configuration with single vertical tail. M = 2.01; $\delta_c = 0°$.

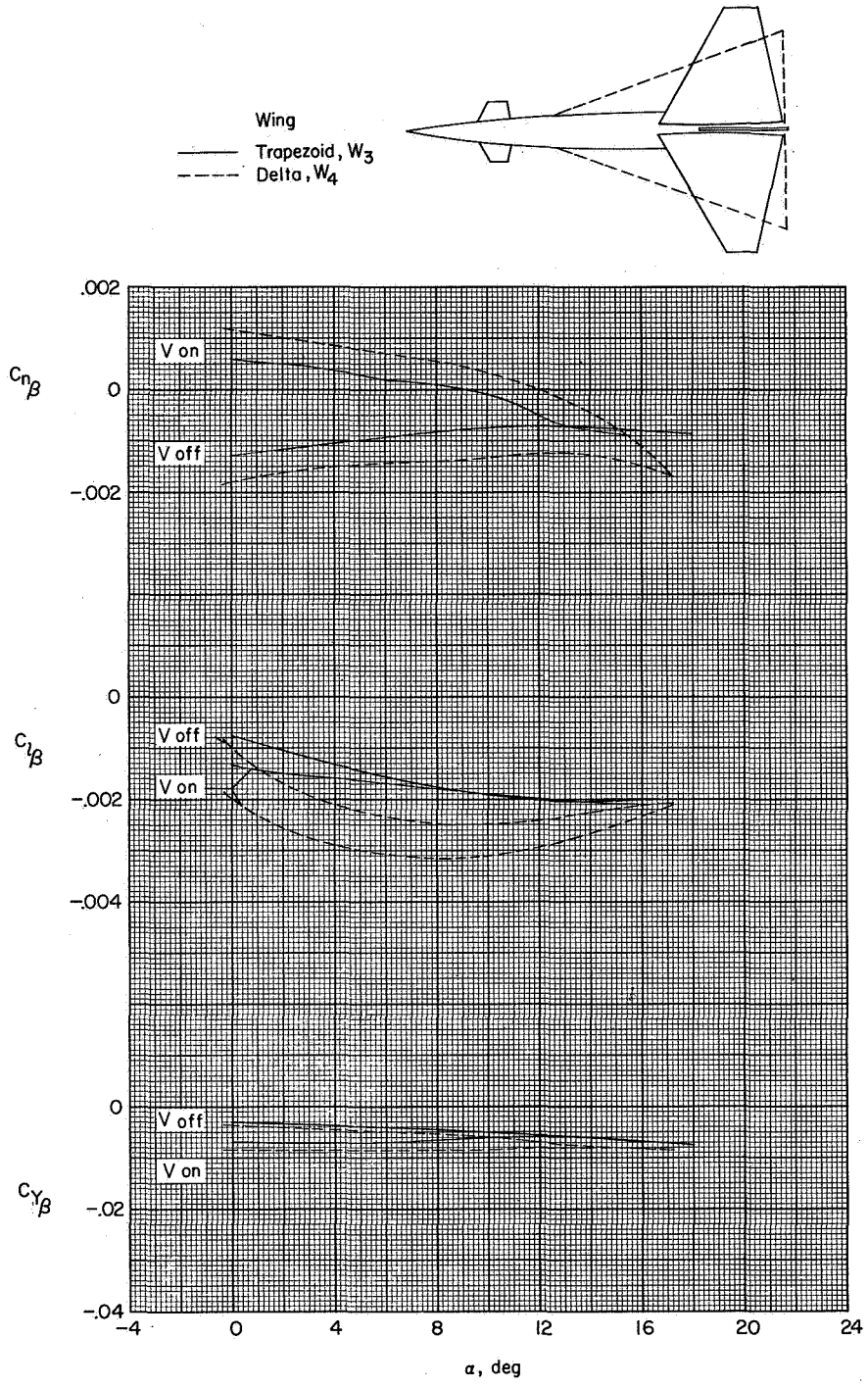

Figure 30.- Effect of wing plan form on sideslip derivatives for high-wing $B_4V_2C_2$ configuration with and without single vertical tail. M = 2.01; $\delta_c = 0^o$.

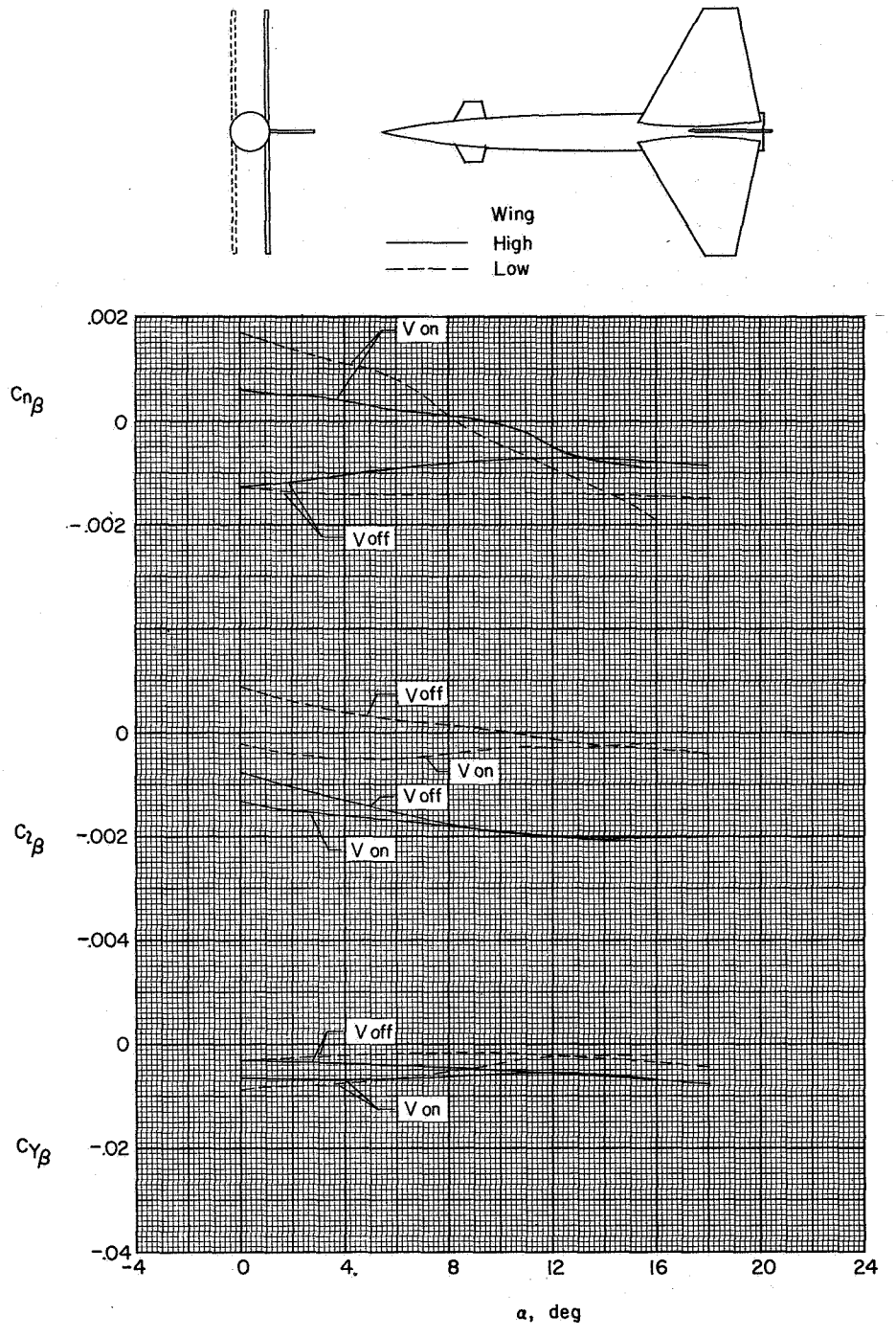

Figure 31.- Effect of wing height on sideslip derivatives for trapezoidal-wing $B_4W_3V_2C_2$ configuration with and without single vertical tail. $M = 2.01$; $\delta_c = 0^\circ$.

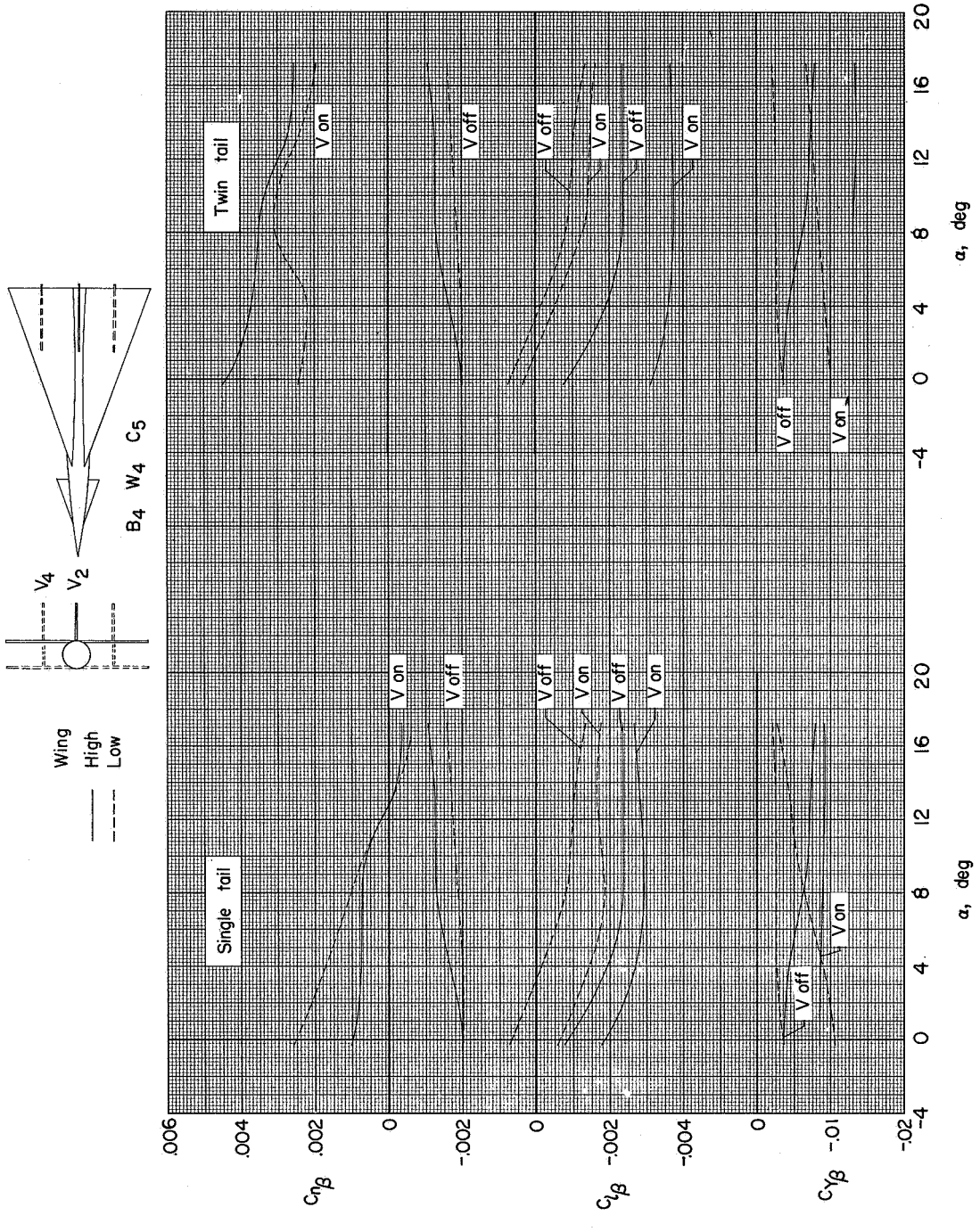

Figure 32.- Effect of wing height on sideslip derivatives for 70° delta-wing configuration with and without a single and a twin vertical-tail arrangement. $M = 2.01$; $\delta_c = 0^c$.

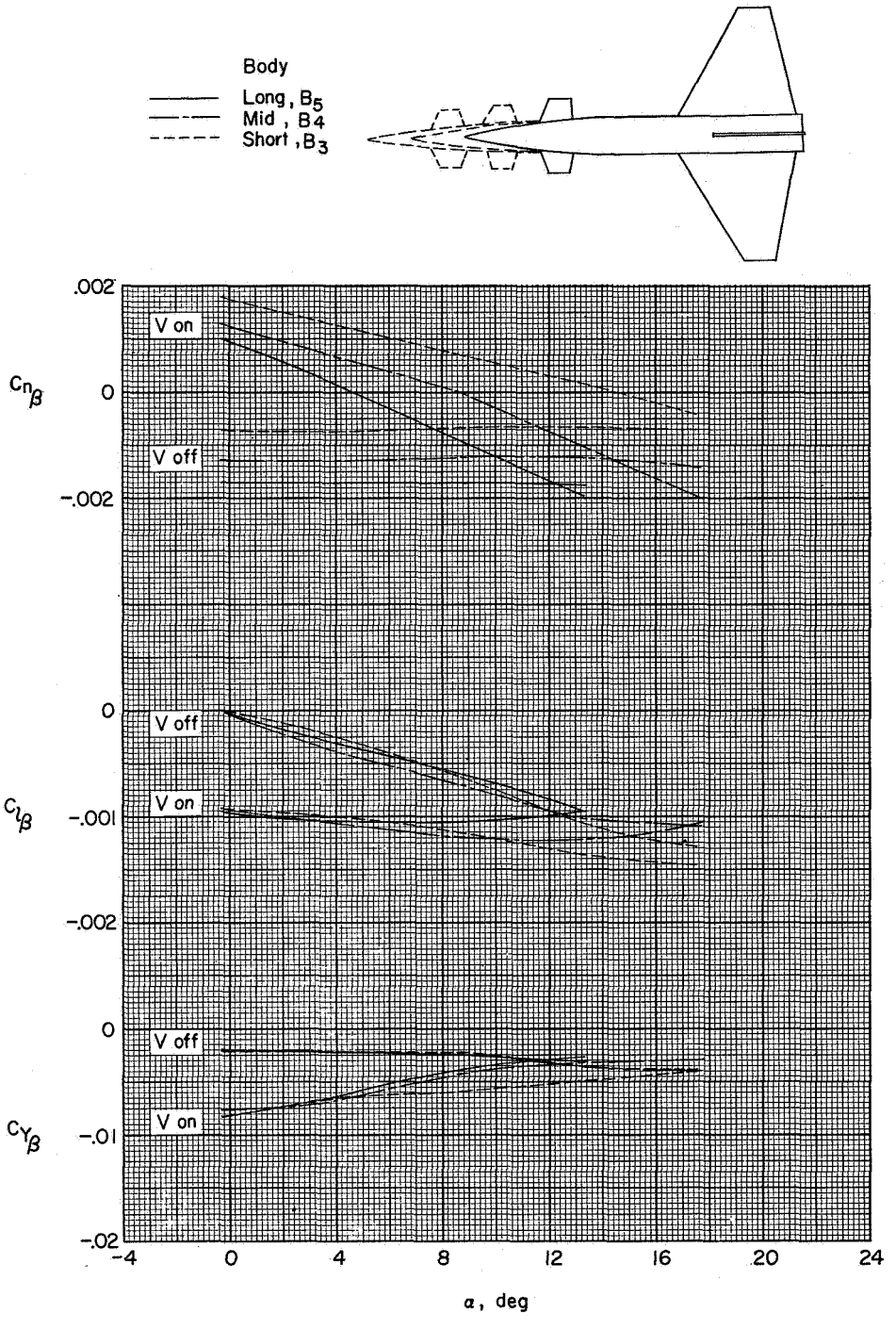

Figure 33.- Effect of body length on sideslip derivatives for trapezoidal-midwing $W_3V_2C_2$ configuration with and without single vertical tail. $M = 2.01$; $\delta_c = 0^o$.

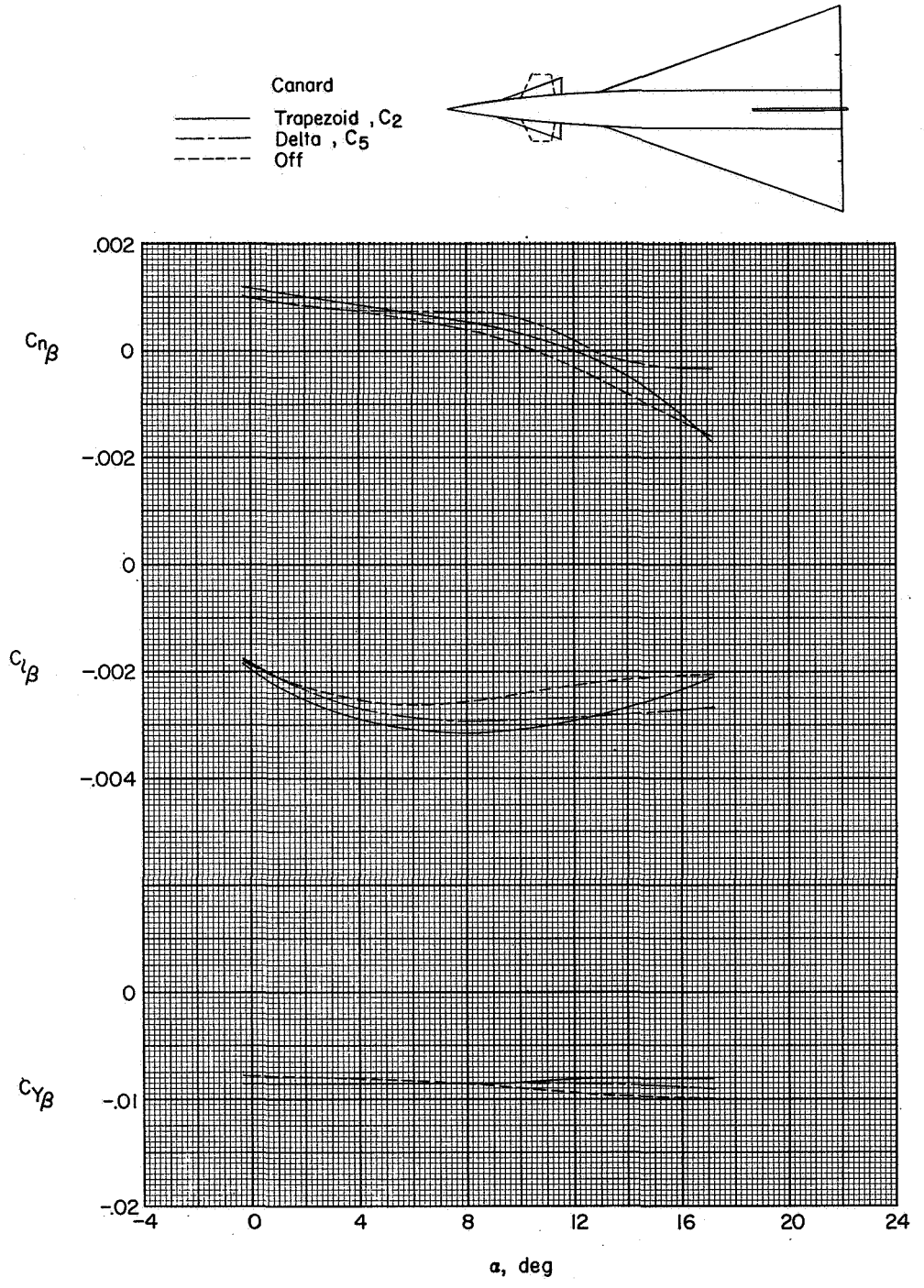

Figure 34.- Effect of canard-surface plan form on sideslip derivatives for 70° delta-midwing $B_4W_4V_2$ configuration with single vertical tail. M = 2.01; $\delta_c = 0°$.

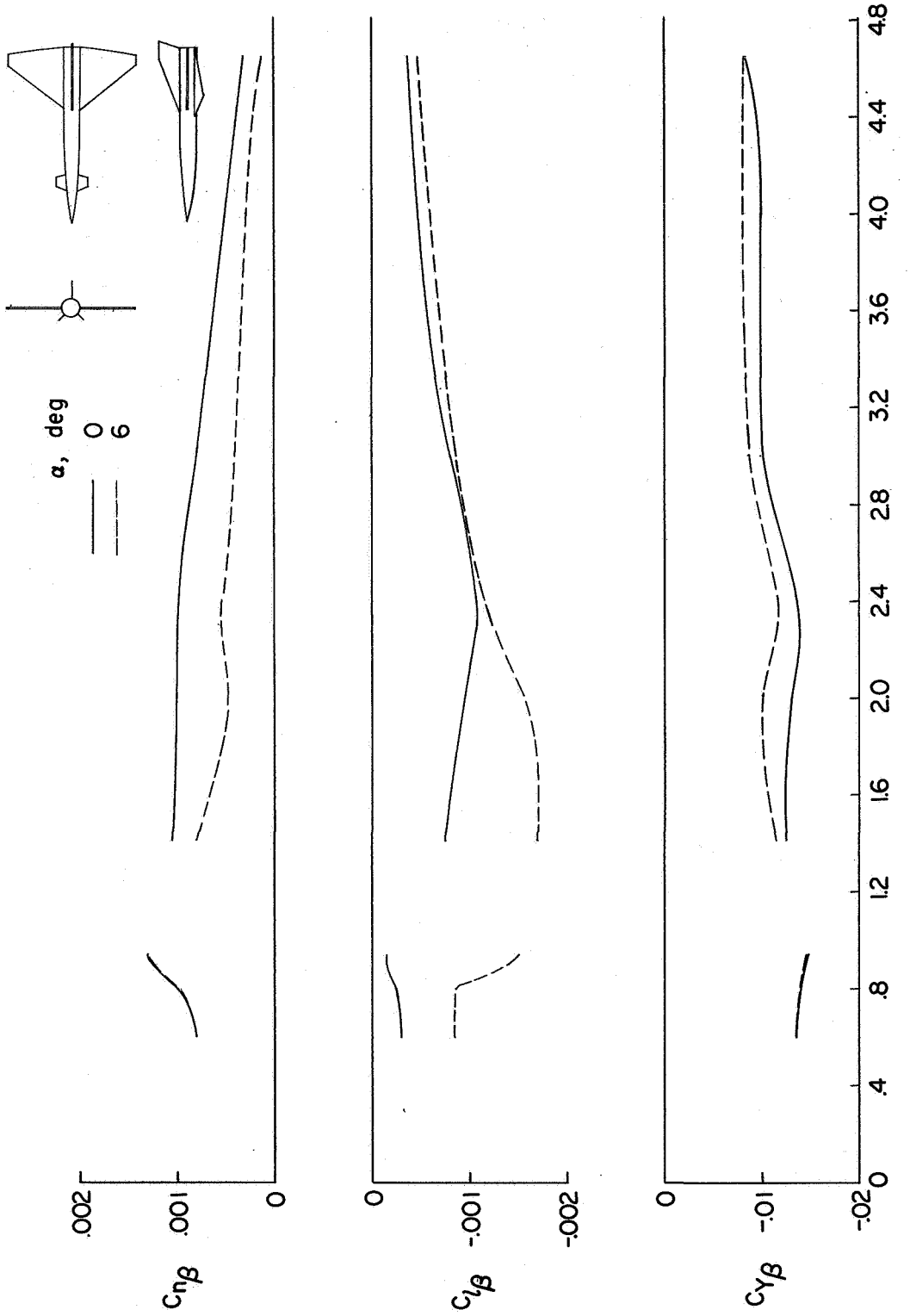

Figure 35.- Variation of sideslip derivatives with Mach number for $B_1W_1V_5C_2U_1$ configuration. $\delta_c = 0^\circ$.